Encyclopedia of Complexity and Systems Science
DOI 10.1007/978-3-642-27737-5_606-1

Earthquakes and Water

Chi-yuen Wang* and Michael Manga
Department of Earth and Planetary Science, University of California, Berkeley, CA, USA

Keywords

Earthquakes; hydrological responses; liquefaction; mud volcano; changes in stream discharge; groundwater flow; transport; temperature and composition

Glossary

Alluvial fan A fan-shaped deposit built up by sediments deposited by a stream that exits from a mountain front onto a plain. Over time the stream and its deposits move across different parts of the fan surface

Aquifers confined and unconfined Aquifers are layers of sediments or rocks with relatively high permeability in which groundwater can move comparatively freely. A confined aquifer is an aquifer bound by impervious sediments or rocks both on its top and on its base. An unconfined aquifer, on the other hand, is one where the upper boundary is the groundwater table that may rise and fall with seasonal changes in precipitation and with the withdrawal of groundwater

Baseflow recession During dry seasons the discharge in a stream is derived from groundwater that flows to the streambed and is called baseflow. Over long dry periods, the baseflow decreases with time. The decrease of stream discharge over time is the baseflow recession

Capillary fringe A layer above the groundwater table where groundwater seeps upward by surface tension (capillary force) to fill pores

Darcy's law The basic law for groundwater flow discovered by Henry Darcy in 1856 through experimentation, which may be expressed in one of the following forms:

$$Q = \frac{KA(h_1 - h_2)}{L}$$

$$q = -K\frac{dh}{dL}$$

where L is the sample length along which water flows h_1 and h_2 (with $h_1 > h_2$) are the hydraulic head at the two

*Email: chiyuen@berkeley.edu

Encyclopedia of Complexity and Systems Science
DOI 10.1007/978-3-642-27737-5_606-1

ends of the sample, A is the cross-sectional area of the sample, K the hydraulic conductivity, and Q the amount of water flowing from the higher end to the lower end of the sample, q is the amount of flow per unit area also known as the Darcy's velocity. The dimension of Q is L^3/t where t is time, those for q and K are both L/t same as velocity. The transmissivity T of an aquifer of thickness b is defined as $T = bK$. The hydraulic conductivity of most rocks is anisotropic and is more properly expressed as a second-rank tensor $\boldsymbol{K}$. Thus, Darcy's law is often written in the following form:

$$\boldsymbol{q} = -\boldsymbol{K} \cdot \nabla h$$

Darcy's law applies only for laminar groundwater flows. Deviation from laminar flow occurs when the Reynold's number ≥5. In most situations, however, groundwater flow is laminar and Darcy's law is valid.

Dynamic stresses Stresses produced by the passage of seismic waves.

Effective stress Experiments show that the mechanical properties of porous solids such as friction and strength, depend on the pressure of pore fluid, and the dependence follows the "effective stress" principle (Terzaghi, 1925) defined as

$$\sigma_{ij}^{\mathrm{eff}} = \sigma_{ij} - \alpha p \delta_{ij}$$

where $\sigma_{ij}^{\mathrm{eff}}$ is the effective stress, p is pore pressure, α an empirical constant (the Biot-Willis coefficient) determined by experiment, and δ_{ij} the Kronecker delta. When the effective normal stress is reduced to zero, faults in rocks slip without friction and sediments lose mechanical strength, i.e., they liquefy.

Effective vertical permeability and effective horizontal permeability A common source of permeability anisotropy in sedimentary basins is layering of sediments or sedimentary rocks of different permeability. Thus parallel to the bedding of the layered rocks, the bulk permeability of the assemblage is given by the arithmetic mean:

$$k_H = \sum_i k_i \left(\frac{b_i}{b_t}\right)$$

where b_i and k_i are respectively, the thickness and permeability of the ith layer and b_t is the total thickness of the layered assemblage. Normal to the bedding, on the other hand, the bulk permeability is given by the harmonic mean:

$$k_V = \left(\frac{b_t}{\sum_i b_i/k_i}\right).$$

Thus the average permeability in the horizontal direction (k_H) is dominated by the most permeable layer,

Encyclopedia of Complexity and Systems Science
DOI 10.1007/978-3-642-27737-5_606-1

while that in the vertical direction (k_V) by the least permeable layer.

Groundwater flow equation

A continuum approach is adopted in deriving the differential equation for groundwater flow where a representative elemental volume is defined that is very much greater than the sizes of the individual pores in rocks and sediments but is very much smaller than the domain of study. Together with Darcy's law and the continuity equation, this approach allows the derivation of the differential equation for groundwater flow:

$$s_s \frac{\partial h}{\partial t} = \nabla \cdot (\boldsymbol{K} \cdot \nabla h).$$

where $\boldsymbol{K}$ is the conductivity tensor and S_s the specific storage defined as

$$s_s \equiv \frac{1}{\rho_f} \frac{\partial (n \rho_f)}{\partial h}$$

with a unit of m^{-1}. In deep sedimentary basins the effect of temperature on the properties of pore fluid may be significant, while the effect of pressure is relatively small and can be neglected.

If permeability is isotropic and the effect of temperature is negligible the flow equation reduces to a linear diffusion equation

$$s_s \frac{\partial h}{\partial t} = K \nabla^2 h.$$

sometimes expressed as

$$\frac{\partial h}{\partial t} = \kappa \nabla^2 h.$$

where κ is the hydraulic diffusivity defined by

$$\kappa \equiv K/s_s.$$

Groundwater level saturated and unsaturated zone

Going down from the Earth's surface, a depth is reached below where the sediments or rocks are saturated with groundwater. This is the local groundwater level (or water table). Above the water table is the unsaturated zone (or the "vadose zone") in which pore water is held in place by adhesion and capillary tension.

Hydraulic head

The hydraulic head h is defined as the sum of the gravitational potential energy related to elevation z and pore pressure P and can be expressed as

$$h = \frac{P}{\rho_f g} + z.$$

The hydraulic head in a confined aquifer is measured by the water level in a well that is opened only to this aquifer. In modern monitoring wells the hydraulic head of aquifers is measured using pressure gauges.

Peak ground acceleration and peak ground velocity

The maximum acceleration and velocity of the ground respectively, during an earthquake as recorded by strong motion seismographs, often used to characterize the intensity of shaking at a given location

Encyclopedia of Complexity and Systems Science
DOI 10.1007/978-3-642-27737-5_606-1

Permeability	The hydraulic conductivity K is a composite of the properties of the transmitting fluid and the porous solid: $K = \frac{\rho_f g k}{\mu}$ where ρ_f and μ are respectively, the density and viscosity of the fluid k is the permeability of the porous solid with dimension m^2 and g is the gravitational acceleration.
Pore pressure	Pressure in the fluids in the pores of sediments and rocks. Elevated pore pressure (above 1 atm) can only occur in saturated rocks and sediments
Poroelasticity	A description of the coupled processes of deformation and pore fluid diffusion in saturated porous elastic solids
Rayleigh waves and Love waves	Two types of waves that travel along the surface of solids. Rayleigh waves include both longitudinal and transverse motions with respect to the direction of wave propagation while Love wave include only transverse motions. Both types of waves are produced by earthquakes and travel along the Earth's surface
Seismic energy density	The total kinetic energy per unit volume in a seismic wave train as recorded by a seismograph at a given location. It is the maximum seismic energy available to do work in a unit volume
Soils	A term commonly used in earthquake engineering in referring to unconsolidated sediments
Static stresses	Stresses produced by the permanent displacement of the crustal blocks across the fault that ruptured during an earthquake
Unconsolidated sediments	Loose sediments that have not been cemented or substantially compacted

Introduction

The subsurface is a complex and heterogeneous environment. It stores much of Earth's fresh water and houses a large portion of the Earth's biosphere and human wastes intended for long-term sequestration. The study of this important but complex system is the subject of a workshop sponsored by the US Department of Energy (2010).

The present paper focuses on a less explored complexity introduced by large earthquakes that change the subsurface properties that, in turn, change subsurface flow and transport.

Earthquakes signify sudden changes in the state of the subsurface. Alterations in subsurface flow and fluid properties are thus not surprising. What *is* surprising is the large amplitudes of some hydrological responses and the great distances over which these responses occur. Shortly after the 2004 M9.2 Sumatra earthquake, for example, groundwater erupted from a hydrological monitory well in southern China, 3,200 km away from the epicenter (Fig. 1), and the water fountain reached a height of 50–60 m above the ground surface when it was first sighted. The earthquake is most likely the cause of the eruption because (1) the two events occurred in close succession, (2) the well has been regularly monitored over a decade and water level in the well was stable before the

DOI 10.1007/978-3-642-27737-5_606-1

Fig. 1 A hydrologic monitory well in China responding to the 2004 M 9.2 Sumatra earthquake 3,200 km away (The picture was taken by Hou Banghua, Earthquake Office of Meizhou County, Guangdong, 2 days after the Sumatra earthquake. Reproduced from Wang and Manga (2010))

earthquake, (3) no pumping or injection occurred near the well at the time of the eruption, and (4) other factors known to change groundwater level, such as earth tides, barometric pressure, or local precipitation, could not have caused the eruption.

Besides being a matter of academic interest, earthquake-induced hydrologic changes also have some practical relevance. For example, groundwater-level changes following earthquakes can affect water supplies (Chen et al. 2012), and it is sometimes necessary to evaluate the causative role of an earthquake in insurance claims for loss of water supply (Roeloffs 1998). Groundwater-level increase during earthquakes may also cause floods (Chen and Wang 2009) and put some underground waste repositories at risk (Carrigan et al. 1991; Roeloffs 1998). Earthquakes can trigger seismicity (Hill and Prejean 2007) and induce liquefaction of the ground that caused great damage to engineered structures (e.g., Seed and Lee 1966). They may also affect oil well production (Beresnev and Johnson 1994), remobilize trapped CO_2 (Deng and Cardenas 2013), and induce the eruption of mud volcanoes (e.g., Manga 2007; Mazzini et al. 2007; Lupi et al. 2013; Rudolph et al. 2013). One related subject not touched in this overview is tsunami – an important topic that is covered in other chapters in this Encyclopedia.

The following paper is divided into four sections. We first summarize some field observations, with emphasis on the unexpected (complexities). This is followed by a section exploring the mechanism of the complexities in earthquake hydrology. We then discuss the practical relevance of earthquake hydrology, such as mud volcano explosion, water resources, and subsurface transport. A brief summary and outlook are given at the end of the entry.

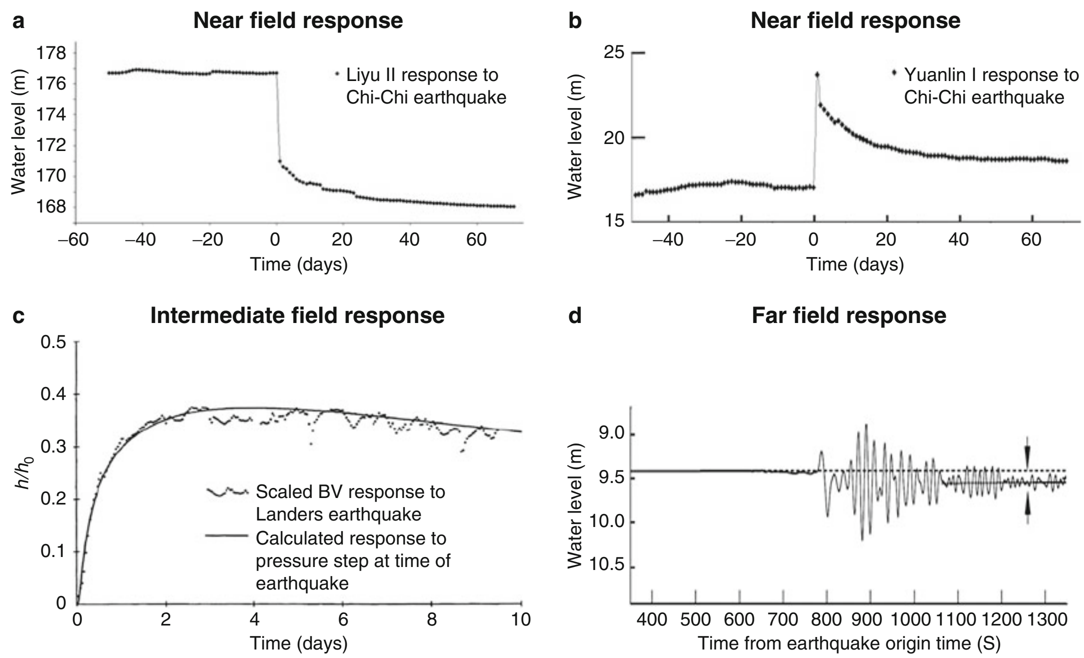

Fig. 2 (**a**) Negative water-level change in the Liyu II well during the 1999 M_w7.5 Chi-Chi earthquake in Taiwan. The well is ~20 km from the hypocenter and ~5 km from the ruptured fault. The steplike coseismic water-level decrease is −5.94 m. (**b**) Positive water-level change in the Yuanlin I well during the 1999 M_w7.5 Chi-Chi earthquake. The well is ~25 km from the hypocenter and ~13 km from the ruptured fault. The steplike coseismic water-level increase is +6.55 m. (**c**) Normalized water level following the 1992 M 7.3 Landers earthquake 433 km from the BV well in central California. *Dots* show observed water-level changes; *solid curve* shows modeled water-level change due to a coseismic, localized pore-pressure change at some distance from the well. (**d**) Groundwater-level oscillations in a well in Grants Pass, Oregon, following the 2002 M7.9 Denali earthquake 3,100 km away. *Arrows* show a 12 cm permanent change in water level (**a** and **b** are modified from Wang and Chia (2008), **b** is reproduced from Roeloffs (1998), and **d** is modified from Brodsky et al. (2003))

Observations

Earthquake-Induced Groundwater-Level Changes

It has been documented since antiquity that earthquakes can cause groundwater levels to change (e.g., Institute of Geophysics – CAS 1976). Instrumental recording of groundwater-level change during earthquakes, however, became available only in the last few decades.

The nature and magnitude of water-level changes after large earthquakes vary with distance from the ruptured fault. For example, in the immediate vicinity (<10 km) of the ruptured fault during the 1989 M7.6 Chi-Chi earthquake in Taiwan, groundwater level abruptly decreases (Fig. 2a; Chia et al. 2001; Wang et al. 2001), followed by an exponential increase or decrease with time. At distances further away but still in the near field (area around the epicenter at distances within ~1 ruptured fault length), water level shows steplike increases (Fig. 2b). The new groundwater level after an earthquake often returns exponentially with time to a new equilibrium (Fig. 2a, b). Plotting the natural logarithm of h versus time t after the earthquake, we find the following linear relation (Wang et al. 2004a):

$$\ln h = a - bt. \tag{1}$$

Encyclopedia of Complexity and Systems Science
DOI 10.1007/978-3-642-27737-5_606-1

The constant b from the fit shows the "recession" of the post-seismic groundwater level. Since h usually decreases with time, a minus sign is placed in front of "b" so that the value of "b" is positive. Although "b" as defined is entirely empirical, it may be shown (Wang et al. 2004a) that it is related to the geometrical and physical characteristics of the aquifer by

$$b \approx \pi^2 \kappa / 4L^2, \tag{2}$$

where κ is the hydraulic diffusivity and L is the characteristic length of the aquifer. After the Chi-Chi earthquake, for example, the values of b evaluated are mostly between 10^{-7} and 10^{-6} s^{-1}, corresponding to a characteristic decay time of 10^1–10^2 days (Wang et al. 2004a).

An interesting spatial distribution of the coseismic groundwater change was revealed after the 1999 M7.6 Chi-Chi earthquake in Taiwan. Taiwan is a mountain belt formed by the collision between the Philippine Sea Plate and the continental margin of the Eurasian plate since the late Cenozoic. The 1999 M7.6 Chi-Chi earthquake, the largest to hit Taiwan in the last century, occurred beneath the foothills of the mountains near a large basin (the Choshui River alluvial fan, 1,800 km^2). About 200 hydrologic wells were installed on the basin for monitoring groundwater resources and, fortuitously, captured the changes of groundwater level and temperature due to the earthquake. Well logs show that the alluvial fan consists of many layers of unconsolidated Holocene gravel, sands, and marine mud, with the proportion of gravel to mud increasing from the coast to the upper rim of the fan. Beneath the alluvial fan is a thick (3–5 km) layer of Pliocene-Pleistocene conglomerates laid down in a collisional foreland basin, which in turn overlies thick Miocene shales. The close proximity to a large earthquake, the relatively simple geology, and the dense network of hydrological stations made the dataset unusually comprehensive and systematic.

In the confined aquifers (i.e., aquifers confined above and below by low-permeability sediments), the rise of groundwater levels after the Chi-Chi earthquake increased in magnitude with distance from the ruptured fault, reaching a maximum of ~5 m at distances of 20–30 km from the fault and then decreased at greater distances (Fig. 3b, c; Chia et al. 2001; Wang et al. 2001). The uppermost, partially confined aquifer, on the other hand, showed no systematic change in groundwater level with distance (Fig. 3a). Such patterns of groundwater response are unexpected because documented ground acceleration shows monotonic decrease with distance from the earthquake source (Fig. 3d). It would thus be natural to expect the change in groundwater level to correspond with the intensity of ground shaking. The unexpected pattern of groundwater-level response reflects strong nonlinearity in the behaviors of soils and sediments under seismic shaking. We will return to this point in section "Mud Volcano Eruptions."

Beyond the near field and at distances up to ~10 ruptured fault lengths (the intermediate field), the change in groundwater level can either be positive or negative, and instead of the steplike response in the near field, the change is more gradual and sustained (Fig. 2c; Roeloffs 1998). When data from a sufficiently large number of wells are collected and examined, the water-level change shows a statistically random occurrence both in sign and magnitude (Wang and Chia 2008). We will return to this point in the discussion of the causal mechanisms in section "Material Nonlinearity and Heterogeneity."

We note here that the above distinction between groundwater-level responses in the near field and the intermediate field is largely based on observations from wells installed in unconsolidated sediments (e.g., Roeloffs 1998; Wang et al. 2001). Recent studies of the groundwater responses to the 2008 M8 Wenchuan earthquake, China, in wells constructed in consolidated sedimentary and fractured crystalline rocks show a statistically random occurrence in sign and magnitude, both in the near field and in the intermediate field (Shi et al. 2014). The new result suggests that the dominant

DOI 10.1007/978-3-642-27737-5_606-1

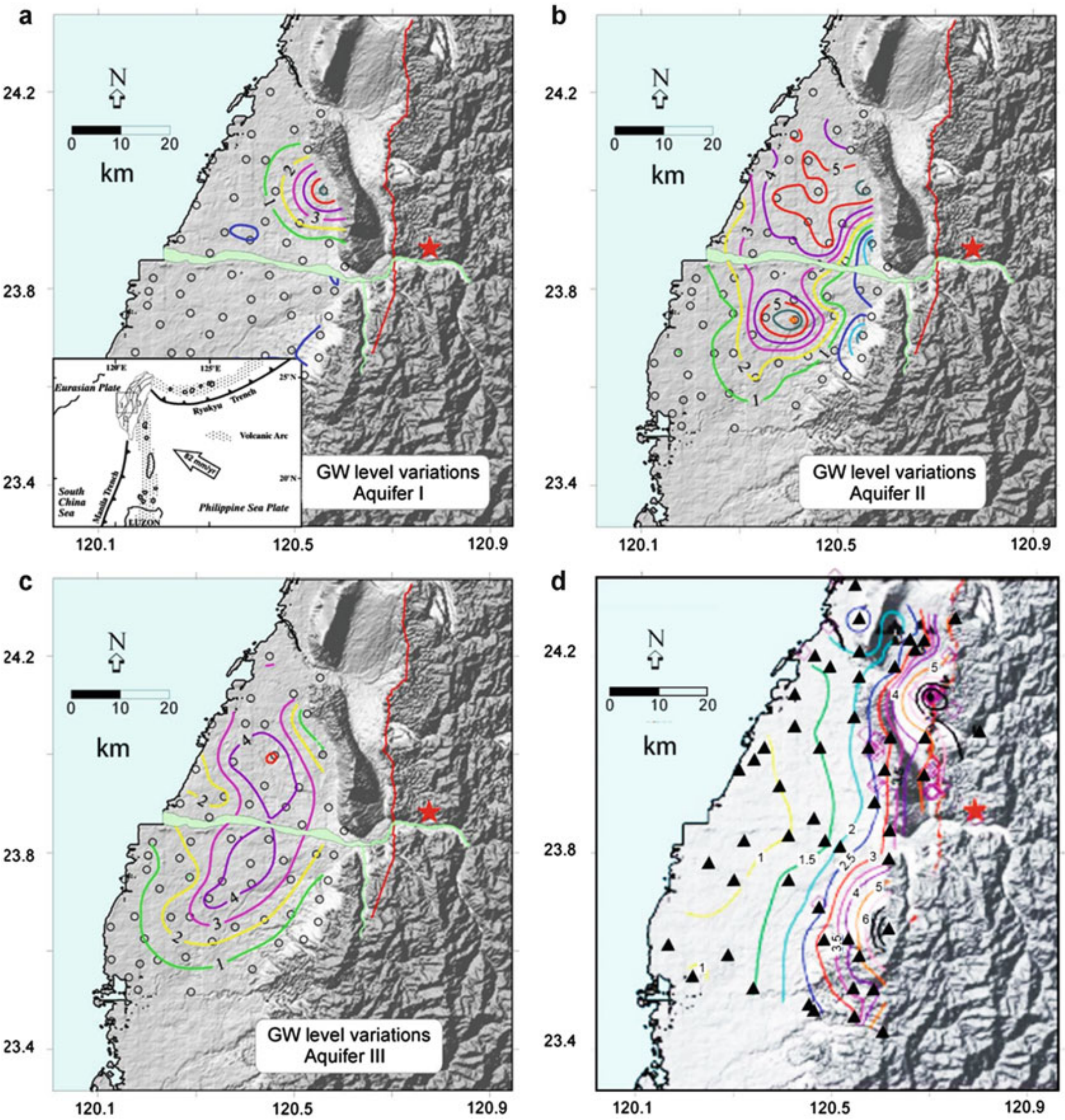

Fig. 3 Distribution of coseismic changes in groundwater level in m (**a**–**c**) and peak ground acceleration in m/s^2 (**d**) over the Choshui River fan during the Chi-Chi earthquake. Circles and contours in (**a**) to (**c**) show locations of groundwater monitoring stations and groundwater-level change in different aquifers, *star* shows epicenter of Chi-Chi earthquake, and discontinuous *red* traces show the ruptured fault; triangles and contours in (**d**) show locations of seismographic stations and the spatial distribution of the horizontal peak ground acceleration (in g) (Modified from Wang et al. 2003). No correspondence is obvious between the spatial patterns of PGA and groundwater-level change

mechanism for groundwater responses in consolidated and crystalline rocks may be different from that for unconsolidated sediments.

In the far field (distances beyond ~10 ruptured fault lengths from the epicenter), seismic waves can cause both transient oscillations and long-term changes in groundwater level. For example, a well in Grants Pass, Oregon, showed groundwater oscillations and permanent change in water level following the 2002 M7.9 Denali earthquake 3,100 km away (Fig. 2d; Brodsky et al. 2003). Following the 2008 M7.9 Wenchuan earthquake, China, some wells in southern Taiwan, located ~2,000 km away, showed water-level oscillations and permanent water-level changes (Wang et al. 2009). In this case, synchronized GPS timing at the wells and broadband seismic stations allowed detailed comparison between groundwater level and seismic waves. Analyses showed that

DOI 10.1007/978-3-642-27737-5_606-1

S- and Love waves, rather than Rayleigh waves, were responsible for initiating water-level oscillations in Taiwan (Wang et al. 2009; Geballe et al. 2011). The finding was surprising because it was generally believed that only Rayleigh waves can cause volumetric strains to induce groundwater flow and oscillations of water-level in wells. It turns out that the unexpected pattern of groundwater-level response may be related to the anisotropic nature of the hydrologic system; we will return to this point in section "Water Resources."

Changes in Streamflow

Changes in stream discharge after earthquakes are among the most interesting hydrologic responses partly because they have often been directly observed. They also represent a response integrated over a large volume beneath the Earth's surface, rather than a point measurement. Streamflow changes have been quantitatively documented for a long time. For example, extensive networks of stream gauges in the western United States, established by the US Geological Survey in the early twentieth century, have collected long and continuous gauging measurements.

The changes in surface hydrology following earthquakes include instant waterfalls created by the earthquake faulting, damming of streams in mountain valleys by landslides and rockfalls, and increased discharge due to avalanching of large quantities of snow from high relief to lower elevations. More interesting and much less well understood are increases in stream discharge that follow earthquakes and persist for an extended duration (commonly several weeks to months) but has no obvious source. This latter type of discharge response is the focus of this section.

A dramatic example of this type was the streamflow increase after the 1989 Mw 6.9 Loma Prieta earthquake (Fig. 4) which occurred during a prolonged drought in California when the stream discharge was very low. After the earthquake, many streams within about 50 km of the epicenter showed increased discharge by a factor of 4–24; the total excess discharge was estimated to be 0.01 km^3 (Rojstaczer et al. 1995).

This total amount, though highly visible, turns out to be quite small in comparison with some estimated excess discharges following other large earthquakes, i.e., 0.7–0.8 km^3 after the M7.5 Chi-Chi earthquake (Wang et al. 2004b), 0.5 km^3 after the M7.5 Hebgen Lake earthquake (Muir-Wood and King 1993), and 0.3 km^3 after the M7.3 Borah Peak earthquake (Muir-Wood and King 1993).

The onset of streamflow increase is coseismic, but the increase can require a few days to reach a maximum, and then gradually decline to reach the pre-earthquake level after several months. Precipitation can easily obscure the earthquake-induced streamflow response when it occurs at the time of, or soon after, an earthquake.

The characteristics of the increased stream discharge following an earthquake may be illustrated on a "baseflow recession curve." After a sufficient lapse of time following the earthquake, the data for the natural logarithm of Q versus time fall closely along a straight line, where Q is the discharge of the stream, i.e.,

$$\ln Q = d - ct. \tag{3}$$

The constant c from the fit is the "recession constant" of the post-seismic stream discharge. Since stream discharge during dry season derives from groundwater discharge, i.e., "baseflow," the constant c also represents the post-seismic recession of the baseflow. Since Q decreases with time and c is defined as a positive value, a minus sign is placed in front of c. While the above relation is entirely empirical, it may be shown (e.g., Manga 2001), by solving the groundwater flow equation under appropriate boundary conditions, that c is related to the aquifer properties by

Encyclopedia of Complexity and Systems Science
DOI 10.1007/978-3-642-27737-5_606-1

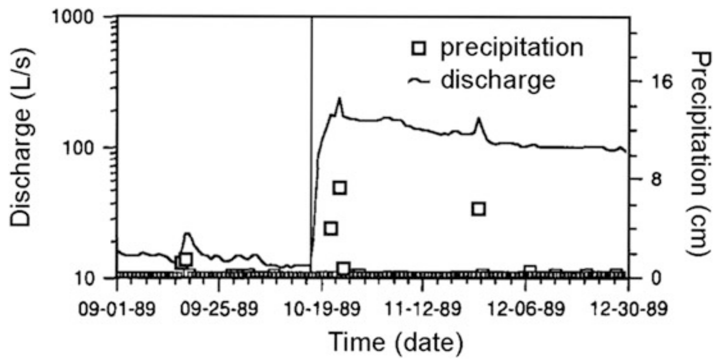

Fig. 4 Discharge in the San Lorenzo River before and after the Loma Prieta earthquake in California. *Vertical line* shows the time of the earthquake; *squares* show local precipitation (Modified from Rojstaczer and Wolf (1992))

$$c \approx \pi^2 \kappa / 4L^2, \tag{4}$$

where, as in Eq. 2, κ is the hydraulic diffusivity and L the characteristic length of the aquifer. Values of c evaluated from the streamflow data after the Chi-Chi earthquake range from 10^{-7} to 10^{-5} s^{-1} (Wang et al. 2004b), similar to the values of b, the recession constant for the post-seismic decline of the groundwater level discussed in section "Earthquake-Induced Groundwater-Level Changes," suggesting that similar processes may control the post-seismic streamflow recession and groundwater-level recession.

Where did the excess water come from? Three hypotheses have been advanced: water is expelled from the crust as a result of coseismic elastic strain (e.g., Muir-Wood and King 1993; Ge and Stover 2000); water is released from the upper crust because of increased fracture permeability (e.g., Rojstaczer et al. 1995); and water is released from coseismic liquefaction or consolidation of loose sediments (Manga 2001; Manga et al. 2003). The different mechanisms imply different processes for groundwater recharge and discharge in earthquake cycles and thus different impacts on geologic processes.

With respect to the first hypothesis, Rojstaczer et al. (1995) showed that if the excess water was expelled from the crust due to coseismic elastic strain, a layer of crust several tens of km thick must have been involved, which would imply changes in groundwater temperature and chemistry not found in the post-seismic stream discharge. Manga et al. (2003) further showed that the discharge of a stream in southern California always increased after earthquakes, irrespective of the signs of the local volumetric strain caused by the earthquakes.

With respect to the second hypothesis, Manga (2001) found that the recession constant c for some streams after earthquakes was the same as before the earthquake. Since c is related to the hydraulic conductivity through Eq. 4 and L, the effective length of the aquifer, is unlikely to change, the finding suggests that the hydraulic conductivity of aquifers did not change after earthquakes.

With respect to the third hypothesis, Wang et al. (2004b) used discharge data from several stream systems over the Choshui River alluvial fan to show that discharges did not change across the alluvial fan where abundant liquefactions occurred during the Chi-Chi earthquake. Instead, large increases of discharge occurred in the stream tributaries in mountains where there were little sediments to liquefy or consolidate. Thus the extra water in the streams did not originate from liquefaction or consolidation but must have originated from the mountains.

Thus, none of the three hypotheses seems to entirely explain the source of the excess stream water after the earthquake. We will return to this point when we discuss the aquifer anisotropy in section "Material Anisotropy."

Encyclopedia of Complexity and Systems Science
DOI 10.1007/978-3-642-27737-5_606-1

Liquefaction During Earthquakes

Liquefaction during earthquakes is a process by which the rigidity of saturated sediments is reduced to zero and the sediments become fluid-like. The process is invariably associated with high pore-water pressure, as evidenced by the ejection of water and sediments to substantial height during liquefaction.

In 373/2 BC, Helice, a coastal town in ancient Greece, disappeared entirely under the sea after a great earthquake as a result of liquefaction and land subsidence. Following the 1964 M9.2 Alaska earthquake, great damage also occurred along the coast near Anchorage, Seward, and Valdez where the slumping of land was caused by the liquefaction of soft clays and sands beneath a gentle slope (Seed 1968). Liquefaction during the 1964 M7.5 Niigata Earthquake, Japan, also caused dramatic damage in the Niigata City. During the 2010–2011 Canterbury earthquake sequence in New Zealand's South Island (including the most damaging 2011 M6.2 Christchurch earthquake), wide-spread and recurrent liquefaction caused damage to thousands of residential properties, at an estimated $1B NZ in economic losses (Quigley et al. 2013).

Undrained Consolidation as a Mechanism for Liquefaction

Spurred by the great liquefaction damage associated with the 1964 Alaskan and Niigata earthquakes, earthquake engineers have carried out extensive research on the mechanism of soil liquefaction in order to predict its occurrence. This work is summarized in several special volumes (e.g., National Research Council 1985; Pitilakis 2007). The engineering approach has been based on the principle of effective stress, first proposed by Terzaghi (1925), where the normal stress in sediments is offset by the pressure in the pore fluids. If pore pressure increases, the effective stress decreases by a proportional amount. Since the mechanical strength of sediments is proportional to the effective stress, a decrease in the effective stress causes the sediments to weaken. During seismic shaking, sediments consolidate. Since the time available is too short for pore water to drain, consolidation proceeds under an undrained condition – thus "undrained" consolidation – and pore pressure in the sediments increases. When pore pressure becomes so high that the effectives stress is reduced to zero, sediments become fluid-like; i.e., they liquefy.

While engineers view "undrained consolidation" as the primary mechanism for liquefaction, we show in the next subsection that earthquake-induced liquefaction also occurs at distances where the seismic energies are far below that required to cause undrained consolidation.

Threshold Distance

Several authors (e.g., Papadopoulos and Lefkopulos 1993; Ambraseys 1988; Galli 2000) noticed that the occurrence of liquefaction is bound by an empirical relation of the form: $\log r = \mathrm{A} + \mathrm{B}\, M$, where r is the maximum distance of liquefaction sites (the threshold distance) from the earthquake source, beyond which liquefaction is not expected, M the earthquake magnitude, and A and B the fitting constants. Using a substantially larger data set than previous studies, Wang et al. (2006) found the following relationship between the bounding distance of liquefaction, r, and earthquake magnitude M:

$$\log r = 0.45M - 1.05 \tag{5}$$

where r is in km (Fig. 5).

Cua (2004) showed that the peak ground velocity (PGV) in southern California attenuates with distance as $1/r^{1.5}$ (for soil sites). Since most energy in ground shaking resides in PGV, the available seismic energy to do work in a unit volume, or the *seismic energy density* e, declines with distance according to $e \sim PGV^2 \sim 1/r^3$. Invoking the classical relation between M and the total

Encyclopedia of Complexity and Systems Science
DOI 10.1007/978-3-642-27737-5_606-1

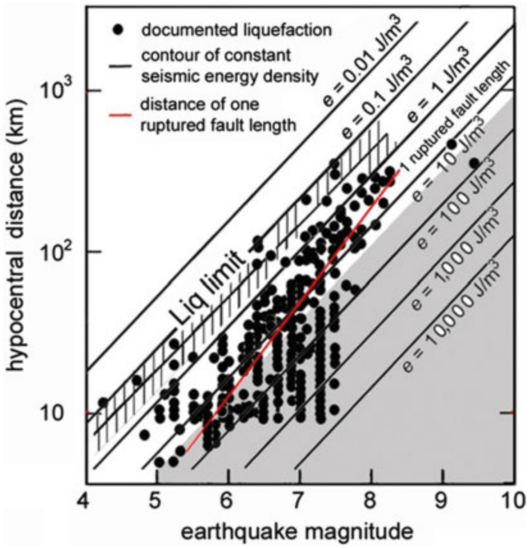

Fig. 5 Global dataset for hypocentral distance of documented liquefactions plotted against earthquake magnitude (Wang et al. 2006). Hachured band marks the threshold distance of liquefaction as a function of earthquake magnitude (Wells and Coppersmith 1994); *red line* is the empirical relation between the epicentral distance of 1 ruptured fault length and earthquake magnitude; the upper boundary of the shaded area corresponds to a contour with a seismic energy density of 30 J/m^3 – the minimum dissipated energy density required to initiate consolidated-induced liquefaction in sensitive soils (Green and Mitchell 2004) (Reproduced from Wang (2007))

seismic energy in an earthquake (Bath 1966), Wang (2007) obtained the following relation among M, r, and e:

$$\log r = 0.48M - 0.33 \log e \; - 1.4 \tag{6}$$

which may be expressed with the seismic energy density as the dependent variable as follows:

$$\log e = 1.5M - 3.0 \log r \; - 4.2 \tag{6'}$$

where r is in km and e in J/m^3.

Several aspects of this relation are noteworthy: contours of constant e plot as straight lines on a log r versus M diagram (Fig. 5); the slope of these lines is nearly identical to that in Eq. 5, i.e., the slope of the empirical relation that delimits the occurrence of liquefaction (Fig. 5); this empirical relation, i.e., the liquefaction limit, is characterized by a constant seismic energy density of 10^{-1} J/m^3 (Wang 2007); this threshold energy is more than two orders of magnitude smaller than the energy required to cause undrained consolidation in sensitive soils (~30 J/m^3, Green and Mitchell 2004). Finally, the near field, defined as the epicentral distance equal to one ruptured fault length (Wells and Coppersmith 1994), lies close to the contour of e ~10 J/m^3 (Fig. 5). Thus, undrained consolidation occurs only in the near field, while liquefaction occurs both within and beyond the near field (Wang 2007; Fig. 5).

Experiment at Wildlife Liquefaction Array

In 1982 the USGS set up a specifically designed field experiment at the Wildlife Reserve in southern California, about 10 km southeast of the Salton Sea, to study liquefaction. Strong motion seismometers and pore-pressure gauges were placed at different depths to allow direct comparison between ground motions and pore pressure (Holzer et al. 1989; Zeghal and Elgamal 1994; Holzer and Youd 2007). In 1987 a M6.6 earthquake (the Superstition Hills earthquake) occurred 31 km away from the Wildlife Reserve and triggered liquefaction at the array. Figure 6a, b shows calculated shear stress and strain from strong motion records during the Superstition Hills earthquake. Figure 6c shows the evolution of pore pressure beneath the array; pore pressure continued to increase after the ground acceleration had abated. It remains a challenge to explain the temporal relation between ground acceleration and pore pressure increase. We will return to this point in section "Material Nonlinearity and Herterogeneity" when discussing the nonlinear response of soils under seismic shaking.

Earthquake-Induced Changes in Groundwater Temperature

Changes in the temperature, odor, and taste of groundwater following earthquakes have long been noted. Progress in our understanding of these processes, however, has been slow, largely because quantitative and systematic data have been scarce. Induced changes in groundwater temperature occur both on land and beneath oceans (Davis et al. 2001), but we focus here on those changes observed on land, where data are relatively plentiful.

Mogi et al. (1989) described temperature changes in an artesian geothermal well in the northeastern part of the Izu Peninsula, Japan. When there are no earthquakes, temperature falls gradually and linearly with time; at the time of earthquakes, however, temperature rises in a stepwise pattern. The authors interpret the gradual decline of temperature during normal times to indicate a decrease in the amount of geothermal water, supposedly due to ongoing precipitation of minerals in underground passageways, slowly blocking the flow of the geothermal water. When a fairly strong earthquake occurs, the seismic waves dislodge the obstacles, and the flow of the geothermal water suddenly increases and temperature suddenly rises.

Mogi et al. (1989) also noticed that, on a plot of earthquake magnitude versus the logarithm of epicentral distance, earthquakes that caused changes in the well temperature are separated from those that did not by a linear relationship. It is interesting to note that the slope of this line is the same as that of Eq. 5, i.e., the threshold relation that delimits the occurrences of earthquake-induced liquefaction. An attempt to unify these relations is described in section "Unified Empirical Relationship."

The dense well network near the epicenter of the Chi-Chi earthquake documented the spatial distribution groundwater temperature changes across a nearby basin (Wang et al. 2013). Groundwater temperature at the screened section of each well was measured using an encapsulated precision thermistor gauge (Aqua TR0LL200) at discreet time intervals. Data from depths less than 100 m are excluded to avoid effects due to surface changes in temperature and recharge. Groundwater temperatures before the Chi-Chi earthquake, projected onto an east-to-west profile as a function of distance from the surface trace of the ruptured fault, are shown in Fig. 7a. Scatter in the data is partly due to the superposition of data from different latitudes and depths onto a single profile. In spite of the scatter, the data show a clear trend of increasing temperature from the upper rim of the alluvial fan on the east to the coast on the west, indicative of active heat transport by groundwater flow across the basin. Figure 7b shows the groundwater temperature in the same wells 2–3 months after the Chi-Chi earthquake. While the groundwater temperature shows the same east-to-west increase, it is slightly lowered near the ruptured fault on the east and raised near the coast relative to measurements before the earthquake. Figure 7c shows the difference between Fig. 7a, b, i.e., the *change* of temperature after the earthquake. Despite the scatter, the data show a clear trend of increase from negative values (temperature decrease) near the eastern rim of the fan near the ruptured fault to positive values (temperature increase) near the coast. This type of earthquake-activated temperature change implies basin-scale flow and transport as a viable mechanism (Wang et al.

Encyclopedia of Complexity and Systems Science
DOI 10.1007/978-3-642-27737-5_606-1

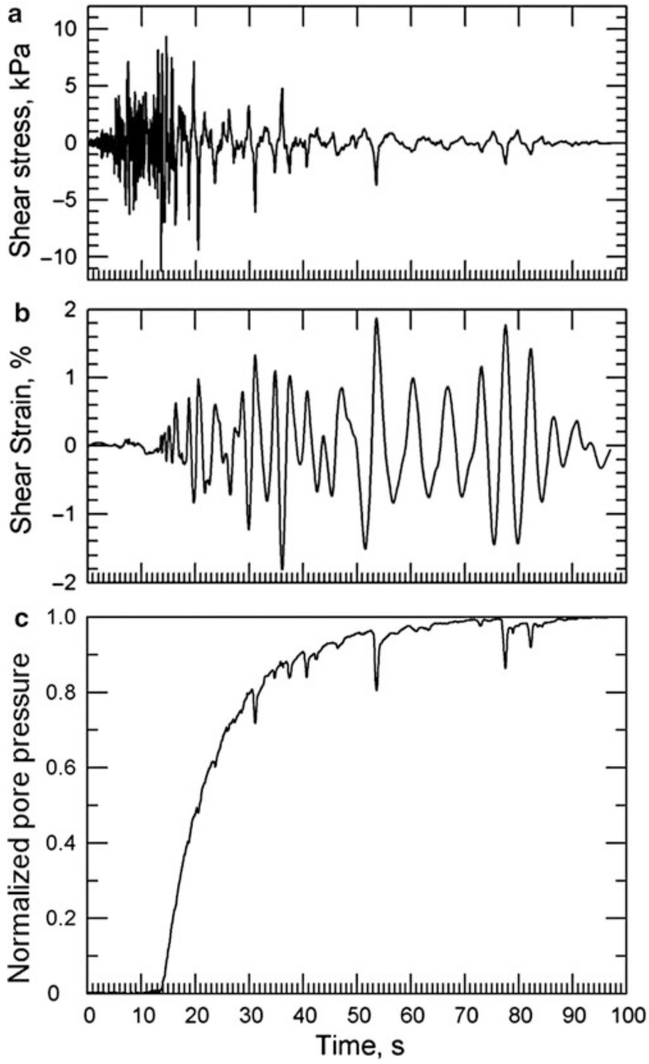

Fig. 6 Shear stress (**a**) and strain (**b**) at the Wildlife Liquefaction Array, CA, during the 1987 Superstition Hills earthquake, calculated from strong motion records. (**c**) Normalized pore pressure beneath the array during ground shaking (Modified from Holzer and Youd (2007))

2013). As discussed in section "Subsurface Transport", it also suggests that earthquake-activated transport processes may extend to depths of several km.

Changes in Groundwater Composition After Earthquakes

Because most measurements of groundwater composition require discrete sampling of water and expensive and time-consuming laboratory analysis, observational data for earthquake-induced changes in water composition are scarce. In a few cases, the composition of stream water and groundwater has been systematically monitored before and after an earthquake. For example, stream water chemistries in the San Lorenzo drainage basin, central California, were monitored at two gauging stations on a biannual basis. Following the Loma Prieta earthquake of 17 October 1989, stream water chemistry showed a marked increase in overall ionic strength, but the overall proportions of the major ions were nearly the same as those before the earthquake (Rojstaczer and Wolf 1992). The ion concentration decreased significantly over a period of several months after the earthquake, to approach the pre-earthquake conditions at both stations.

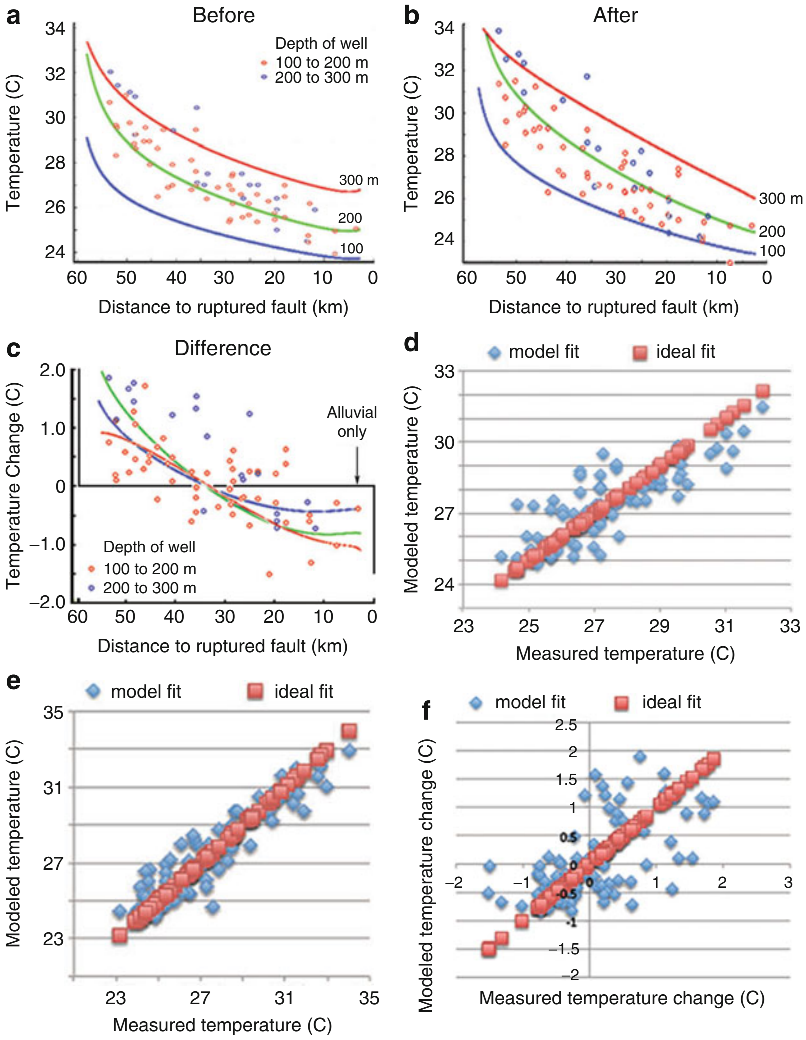

Fig. 7 (**a**) Groundwater temperature in wells on the Choshui alluvial fan ~7 months before the Chi-Chi earthquake. *Circles* are observed temperatures; different colors show measurements made at depths between 100 and 200 m and between 200 and 300 m, as indicated in the figure. *Curves* show simulated groundwater temperatures before the earthquake at 100, 200, and 300 m below the surface (see text for description). (**b**) Groundwater temperature 2–3 months after the earthquake. *Circles* are measured temperatures, and *curves* are simulated temperatures 2–3 months after the earthquake. (**c**) Changes in groundwater temperature after the earthquake (i.e., difference between **b** and **a**). *Circles* are measured values, and *curves* show simulated temperature change 2–3 months after the earthquake. *Black curve* shows simulated temperature change if enhanced permeability is restricted to the upper few 100 m of sediments (see text for explanation). (**d**) and (**e**): Plots of simulated temperatures against measured temperatures before and after the earthquake, respectively (*diamonds*). (**f**): Plot of the difference between simulated temperatures before and after the Chi-Chi earthquake against the difference between measured temperatures before and after the earthquake (Reproduced from Wang et al. (2013))

In Iceland, weekly samples were collected from a borehole located in a fault zone, starting in July 2002. Claesson et al. (2004, 2007) reported 12–19 % increases in the concentrations of B, Ca, K, Li, Mo, Na, Rb, S, Si, Sr, Cl, and SO_4 in the groundwater and decreases in Na/Ca and the oxygen and hydrogen isotopic anomalies 2–9 days after a M5.8 earthquake on 16 September 2002 with epicenter ~90 km north of the borehole. The chemical changes recovered gradually over the subsequent 2 years.

Encyclopedia of Complexity and Systems Science
DOI 10.1007/978-3-642-27737-5_606-1

In Taiwan, groundwater chemistry is measured during routine well maintenance (Wang et al. 2005). After the Chi-Chi earthquake, the oxygen isotopes in the aquifer shifted significantly towards lighter values. The shift decreased with time, and the isotopic composition returned to pre-earthquake values in the summer of 2001, nearly 2 years after the Chi-Chi earthquake. This recovery time is similar to that found by Claesson et al. (2007) for the earthquake-induced chemical changes in well water in Iceland but significantly longer than that reported by Rojstaczer and Wolf (1992) for the earthquake- induced chemical changes in stream water in central California. Part of this difference may be due to the flushing of stream water by surface runoff during the rainy season following the Loma Prieta earthquake.

Response of Mud Volcanoes

Mud volcanoes are features that erupt a mixture of water, gas, and solid particles to the surface. These materials may originate from depths of up to a few kilometers and can create edifices up to a few 100 m high and a few kilometers in diameter. They are of scientific interest because of their role in natural hydrocarbon cycling (Kopf 2002; Etiope et al. 2011) and as a window into vertical fluid transport in the crust (Miyakawa et al. 2013). Occasional paroxysms may also present a local geological hazard.

Eruptions in response to earthquakes have been documented since Pliny (79), and there are long records of earthquake responses from Italy (Bonini 2009), Azerbaijan (Mellors et al. 2007), and Japan (Chigira and Tanaka 1997). A compilation of eruptions that occur within a few days of earthquakes shows that the distance over which mud volcanoes respond, for a given earthquake magnitude, is similar to the distance over which liquefaction occurs and over which changes in streamflow have been documented (Manga and Brodsky 2006; Mellors et al. 2007). However, mud volcanoes near the Wildlife Liquefaction Array discussed in section "Liquefaction During Earthquakes" have erupted in response to earthquakes that did not induce liquefaction at the study site (Rudolph and Manga 2010).

In order to identify whether static stress changes influence eruptions, Manga and Bonini (2012) calculated changes in unclamping stresses on dikes that feed mud volcanoes in the Northern Apennines, Italy. Figure 8 shows the predicted changes following two earthquakes located in the intermediate field. The first earthquake produced stresses that acted to unclamp feeder dikes, and all three mud volcanoes increased their discharge. After the second earthquake, only the one mud volcano that experienced unclamping stresses responded. The conclusion is thus that unclamping (opening) dikes feeding the eruptions increases discharge. This is not unexpected, but it is noteworthy that the static stress changes are small, less than 0.1 bar.

Other mud volcanoes may respond to seismic waves rather than static stress changes. Rudolph and Manga (2012) documented responses and nonresponses of mud volcanoes in the Imperial Valley, California, to several earthquakes in the intermediate field. They found no correlation with the amplitude of static stress changes. There was also no correlation with the peak ground velocity or the duration of shaking. Instead, the best correlation was found with the amplitude of ground motion at long periods, <10 Hz. It should be noted that both of these studies are based on a limited number of data.

While the number of events is too small to permit a statistical test of these hypotheses, Bonini et al. (2014) subsequently use historical data to support the original inference in Manga and Bonini that unclamping feeder dikes is the mechanism. On the other hand, the same paper concludes that triggering occurs through many processes, including dynamic stresses and unclamping dikes.

In summary, mud volcanoes appear to respond to both static and dynamic stresses. Identifying the origin of the responses is challenging both because of the limited number of observations (less than

Encyclopedia of Complexity and Systems Science
DOI 10.1007/978-3-642-27737-5_606-1

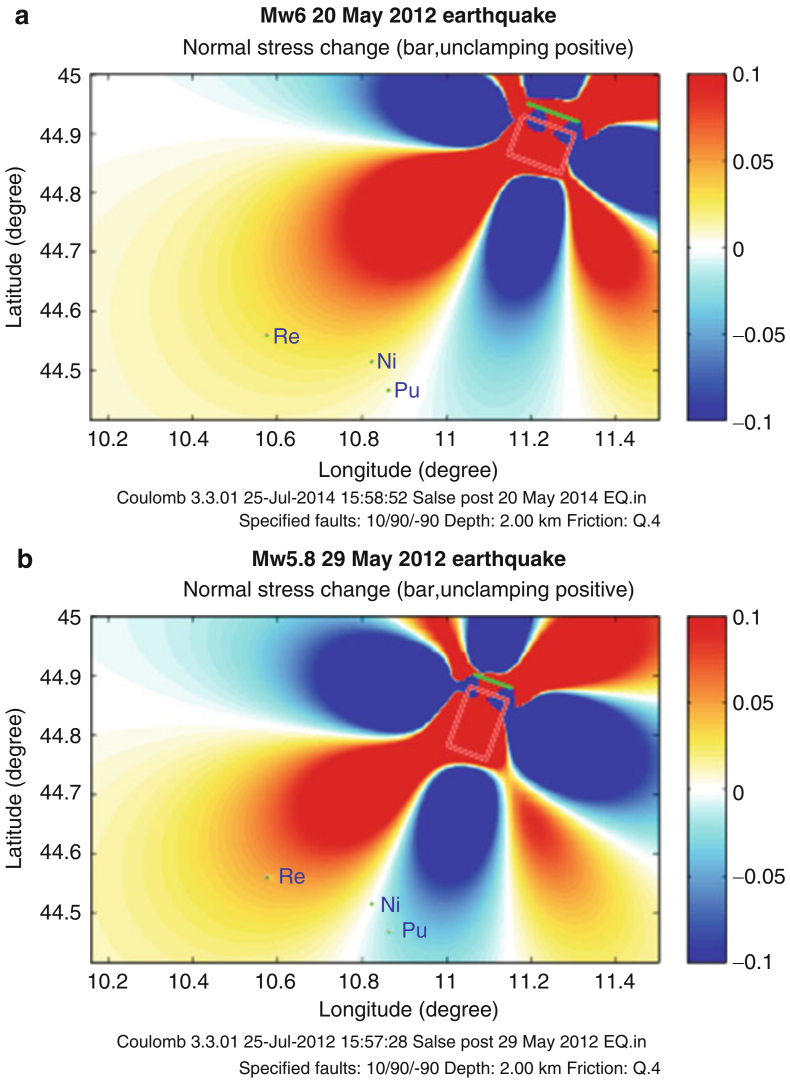

Fig. 8 Changes in stress acting normal to the feeder dikes under mud volcanoes in the Northern Apennines, Italy. *Red* indicates stresses that act to unclamp the dikes. Location of three mud volcanoes, Regnano (Re), Nirano (Ni), and Puianello (Pu), shown with the *small dots*. After the 20 May event, all three mud volcanoes responded, but after the 29 May event, only Regnano increased its discharge (From Manga and Bonini (2012))

40 documented responses) and because many of the key processes may occur at depths of 10s–1,000s of meters below the surface.

Response of Geysers

Geysers intermittently erupt mixtures of liquid water and vapor. Responses to earthquakes, identified as changes in the interval between eruptions, have been documented at geysers in California (Silver and Vallette-Silver 1992) and Yellowstone National Park (Marler 1964; Rinehart and Murphy 1969; Hutchinson 1985; Husen et al. 2004). Geysers are most notable in the context of earthquake responses because of their extreme sensitivity – geysers in Yellowstone changed their eruption behavior following the 2002 magnitude 7.9 Denali earthquake with an epicenter 3,100 km away (Fig. 9).

Our ability to decipher why geysers are so sensitive to earthquakes is limited by our understanding of how and why geysers erupt. Are the eruptions driven by boiling in the conduit caused by

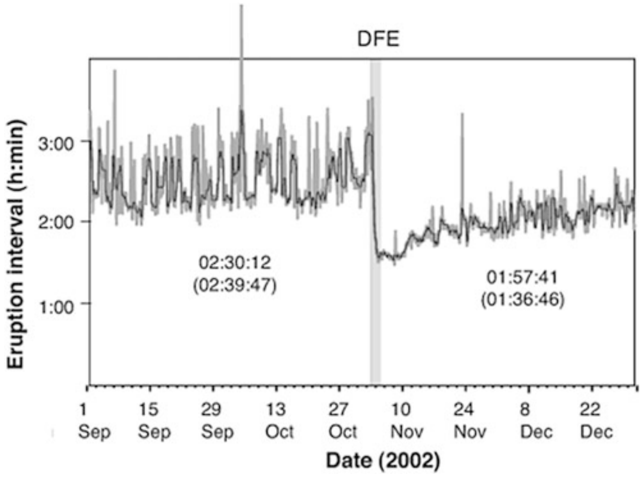

Fig. 9 Response of Daisy Geyser, Yellowstone National Park, to the magnitude 7.9 Denali earthquake (time indicated by the *vertical line*) located 3,100 km from the geyser. Changes in the interval between eruptions persist for $>$ 1 month. The two sets of numbers show the median eruption intervals prior to and after the earthquake, in hour, minute, and second format. The numbers in parentheses are averages over a few days; the numbers above the parentheses are averages over weeks (Modified from Husen et al. (2004))

removing water from the top (Bunsen 1847) or by accumulating steam and overpressure at depth (e.g., Steinberg et al. 1982a)? Are eruption intervals controlled by conduit and matrix permeability (Ingebritsen and Rojstaczer 1993) or the geometry of subsurface cavities (Belousov et al. 2013)? Does water become superheated prior to eruption (White 1967; Rinehart 1980; Steinberg et al. 1982b)? These questions remain the subject of active research, and the response of geysers to earthquakes may provide constraints on models for how natural geysers work.

One key observation is that post-seismic changes in the interval between eruptions persist for weeks to months, as shown in Fig. 9. This cannot be explained by seismic waves nucleating bubbles and initiating the boiling of metastable water (Steinberg et al. 1982b). Instead, some part or parts of the geyser system must have experienced long-lived changes. Changes in permeability induced by seismic waves are often invoked to explain changes in eruption behavior (Ingebritsen and Rojstaczer 1996).

Unified Empirical Relationship

Wang and Manga (2011) attempted to unify the various hydrological responses into a coherent picture. As noted in section "Earthquake-Induced Changes in Groundwater Temperature," earthquakes that caused changes in the temperature of artesian geothermal wells are separated from those that did not by an empirical linear relation between earthquake magnitude and the logarithm of epicentral distance (Mogi et al. 1989), and the slope of this relation is the same as that of the threshold relation that delimits the occurrence of earthquake-induced liquefaction (Eq. 5). Other types of hydrological responses also appear to be delimited by similar relationships (Fig. 10), some require greater seismic energy density (e.g., liquefaction, mud volcano eruption, streamflow changes), while others require less (e.g., well-level changes, changes of geothermal well temperature). It is important to note that most mud volcano eruptions are not triggered by earthquakes; the examples shown in Fig. 10 include only clearly identified triggered eruptions. Each type of hydrologic response spans four or more orders of magnitude of the seismic energy density values. Such scatter is expected for two reasons. First, if triggering is a threshold process, then for all distances up to the threshold, we might expect triggering to be possible. Second, because the

Encyclopedia of Complexity and Systems Science
DOI 10.1007/978-3-642-27737-5_606-1

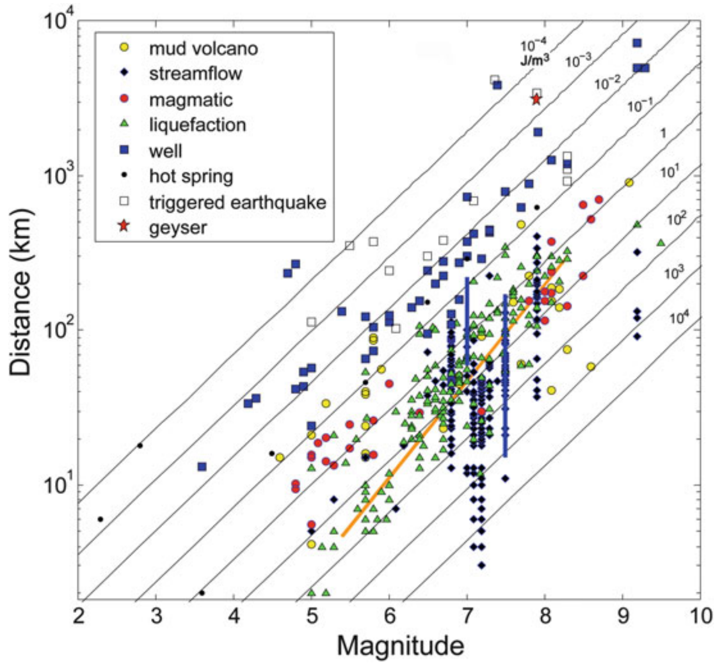

Fig. 10 Distribution of earthquake-induced hydrologic changes as functions of earthquake magnitude and epicentral distance. Data tabulated in Wang and Manga (2010). Also plotted are the contours of constant seismic energy density e, in J/m^3, which is the seismic energy in a unit volume responding to the seismic wave train; it thus represents the maximum seismic energy available to do work at a given location during the earthquake. Note that some data from artesian geothermal wells shown here were not used by Mogi et al. (1989) in defining their linear M versus log r relationship for earthquake- induced temperature changes (Reproduced from Wang and Manga (2011))

hydromechanical properties of rocks and sediments are highly variable, the range of sensitivity to seismic shaking may be large. The threshold seismic energy density for specific types of hydrological response corresponds to that required to initiate responses in the most sensitive sediments or rocks.

Part of the differences in the threshold energy between different hydrological responses may be a result of incomplete data. But data for most of the responses summarized in Fig. 10 are abundant and come from a wide range of geological settings. Thus, the differences in the threshold energy among the different hydrologic responses may be significant, and the empirical relation (Eq. 6) may provide a physically meaningful, general metric to relate and compare the various hydrologic responses.

Thus, starting at a threshold energy density of ~10^{-4} J/m^3, seismic waves may dislodge minute clogs from fractures to enhance permeability and redistribute pore pressure, resulting in changes in groundwater level in the most sensitive wells and changes in geothermal well temperature. Geysers have long been known to be particularly sensitive to earthquakes, as manifested by changes in the time interval between eruptions (Ingebritsen and Rojstaczer 1993). Some geysers in Yellowstone National Park, for example, have responded to seismic energy density as small as 10^{-3} J/m^3 (Fig. 10; see also Husen et al. 2004). Given the limited number of data, however, we are unable to confirm whether a M versus log r relationship may also apply to geysers. Increasing seismic energy density may remove larger blockages from fractures to allow more efficient groundwater flow and cause noticeable changes in groundwater level in less sensitive wells and in geyser eruption frequency. Continued increase in pore pressure and removal of blockages act to degrade the soil stiffness during each seismic cycle until $e \sim 10^{-1}$ J/m^3 when sensitive soil liquefies. Since mud volcanoes triggered by earthquakes require the liquefaction or fluidization of the erupted material, it is natural to expect that earthquake-triggered mud volcanoes and liquefaction are created by the same process and thus constrained by a similar threshold of seismic energy density (Fig. 10).

Complexity

In this section we show that some unexpected hydrological responses to earthquakes may originate from the nonlinear and heterogeneous properties of rocks/sediments, their anisotropic and time-dependent nature, and the fluids residing in the solid matrix. We also show that the responses may depend on the frequencies of the impinging seismic waves. Finally, the interaction and feedback among different processes may introduce additional complexities.

Material Nonlinearity and Heterogeneity

Undrained Consolidation and Other Mechanisms

One important finding from soil mechanics experiments is that, when subjected to cyclic loading, saturated soils undergo undrained change of volume, where solid grains rearrange their relative positions, resulting in either dilatation or compaction depending on the differential stress level. Since the period of loading is short compared with the time required for pore fluid to escape, the process is "undrained."

Through cyclic loading experiments, Luong (1980) showed that if the differential stress level exceeds a characteristic threshold, soils tend to dilate; if cyclically sheared below this threshold, soils tend to consolidate. Using this experimental result, Wang et al. (2001) explained the unexpected pattern in groundwater-level changes after the Chi-Chi earthquake (Fig. 3b, c). In the immediate neighborhood of the ruptured fault, ground shaking was strong, and the differential stresses exceeded the threshold; sediments dilated, causing water level to drop (Fig. 2a). Away from the ruptured fault but still in the near field, the differential stresses were below the threshold, and sediments undergo consolidation, causing water level to rise (Fig. 2b). In between, soils are in a "critical state" with no volumetric change; thus, water level remains unchanged. These responses occur abruptly since consolidation (or dilation) occurs right around the wells.

Another important finding from soil mechanics experiments is that, for a variety of saturated sediments under a broad range of confining pressures, undrained consolidation occurs only when shear strain exceeds a threshold of 10^{-4} (Dobry et al. 1982; Vucetic 1994; Hsu and Vucetic 2004, 2006). Green and Mitchell (2004) also found that a minimum dissipated energy density of 30 J/m^3 is required to cause liquefaction through undrained consolidation in the most sensitive soils. Wang and Chia (2008) further showed that the dissipated energy density required to initiate undrained consolidation ranges from 0.1 to 10 J/m^3. Comparing these results with the maximum available seismic energy density to do work (Fig. 5), Wang (2007) showed that undrained consolidation may be a viable mechanism for liquefaction and water-level changes only in the near field. Beyond the near field, the seismic energy density is too low to initiate undrained consolidation. Thus, the occurrence of liquefaction in the intermediate field (Fig. 5) and the gradual and sustained change of groundwater level (Fig. 2c) require different explanatory mechanisms (see also section "Material Heterogeneity").

Beyond the near field, static poroelastic strain is too small to account for the observed hydrologic changes (Wang and Manga 2011; Manga and Wang 2013). Furthermore, static strain often predicts the wrong sign for the observed groundwater-level changes even in the near field (Wang et al. 2001; Koizumi et al. 2004) and cannot explain the consistent groundwater level increases in the BV well in central California (Roeloffs 1998) or the consistent streamflow increases in Sespe Creek (Manga et al. 2003), southern California, in response to multiple earthquakes of different mechanisms and orientations.

Mogi et al. (1989) first suggested that seismic waves can dislodge obstacles from geothermal well passageways to enhance permeability and cause coseismic increases in temperature (section "Earthquake-Induced Changes in Groundwater Temperature"). The same mechanism was used to explain the sustained changes in groundwater level (Roeloffs 1998; Brodsky et al. 2003) and the increase in stream discharge (Rojstaczer et al. 1995; Wang et al. 2004b) after large earthquakes. Changes in the eruption frequency of geysers can also be caused by changes in permeability of the conduit and/or surrounding matrix (Ingebritsen and Rojstaczer 1993). Elkhoury et al. (2006) showed, through analysis of the tidal response of groundwater level, that seismic waves can indeed significantly enhance the permeability of shallow crust and the magnitude of this enhancement increases with peak ground velocity (*PGV*). Other authors (e.g., Roeloffs 1998) noticed that, at a given well, the amplitude of the sustained groundwater-level change increases in proportion to the increased *PGV*. This may be expected since greater *PGV* is associated with more vigorous shaking and may thus clear more blockages from fluid passageways, resulting in greater increase in permeability and more efficient redistribution of pore pressure. Finally, enhanced permeability is consistent with the gradual and persistent changes in groundwater level observed in the intermediate field of an earthquake (Roeloffs 1998) and the statistically random occurrence of the signs and magnitude of such changes (Wang and Chia 2008). It appears that enhanced permeability in the shallow crust may be a common mechanism for a broad spectrum of hydrologic responses in the intermediate and far fields.

In their analysis of ground motion and pore-pressure change at the Wildlife Liquefaction Array during the 1987 Superstition Hill earthquake (Fig. 6), Zeghal and Elgamal (1994) noticed that the buildup of pore pressure was accompanied by progressive softening of sediments. The time histories of shear stress and shear strain calculated from the ground motion records show that large cyclic shear strains, with amplitude up to ~2 % and long period (~5.5 s), continued to affect the site several tens of seconds after the high-frequency acceleration had abated, leading to the eventual liquefaction. Holzer and Youd (2007) interpret the sequence of events as a result of undrained consolidation under seismic loading.

Wang and Manga (2010) point out, however, that the distance between the Wildlife Reserve Array and the epicenter of the M6.6 Superstition Hills earthquake (31 km) is beyond the near field of the earthquake (<20 km; Fig. 5); thus, the seismic energy density at the Wildlife Reserve Array at the time of the earthquake may have been too small to induce undrained consolidation, even in the most sensitive sediments (Wang and Chia 2008). Furthermore, the increase in pore pressure at the Wildlife Reserve Array during the Superstition Hills earthquake was gradual and sustained (Fig. 6c), suggestive of pore-pressure diffusion from a nearby source due to enhanced permeability (see section "Material Heterogeneity").

In both hypotheses, liquefaction at the Wildlife Reserve Array is the culmination of a complex sequence of interactions among ground shaking, sediment deformation, and pore-pressure redistribution and/or local buildup. An increase in pore pressure weakens the sediment framework; this leads to greater deformation of the sediments. Continued increase in pore pressure may occur due to enhanced permeability connecting the sediments to nearby sources or by continued consolidation. This process continues at low frequency and very small shear stresses until the sediments liquefy.

It remains to be shown that seismic waves with energy densities as small as ~10^{-4} J/m^3 can enhance permeability. Numerical simulations (Wiesner 1999) show that, at low flow velocity, clay particles suspended in water form flocculated deposits and effectively block flow in fractures. Such blockages are non-Newtonian and have a yield strength arising from the bonds among clay particles (Coussot 1995). The yield strength is equivalent to a threshold energy density required to disrupt the bonds among clay particles. For several different clays, this threshold energy density is 10^{-3} J/m^3 for fluids with a few percent of solid fraction (Coussot 1995). It may become even lower under oscillatory seismic loading. Thus, for solid fraction less than 10^{-1}, seismic waves with energy density as low as ~10^{-4} J/m^3 may break up clay networks in fractures to enhance permeability, resulting in greater flow. Increased flow, in turn, may break up more clay networks to create greater permeability, a positive feedback process. Enhanced groundwater flow in Iowa after the 2002 M7.9 Denali earthquake, some 5,000 km away, flushed colloidal particles from local aquifers to an extent sufficient to discolor well waters.

Material Heterogeneity

One manifestation of the complexity of Earth's upper crust is its heterogeneous materials, often shown on geologic maps as different rock types, geologic histories, and structures. Through laboratory experiments, geologists and earthquake engineers have documented the highly variable hydromechanical properties of different rocks and sediments. Permeability of different earth media, for example, varies over 16 orders of magnitude. In light of this variability, it is perhaps not surprising that the seismic energy required to cause different hydrological response to earthquakes ranges across several orders of magnitude (Wang and Manga 2011) and that the occurrences of liquefaction after earthquakes are highly uneven.

As discussed in sections "Material Nonlinearity and Herterogeneity", the seismic energy density beyond the near field is too small to cause undrained consolidation, even in sensitive soils; thus, the occurrence of liquefaction at larger distances (Fig. 5) requires explanation. Here we offer a qualitative explanation based on the heterogeneity of material properties in sedimentary and volcanic deposits. Pore pressure in sedimentary basins is often heterogeneous and occurs in "compartments" separated by impervious rocks, i.e., "seals" (Ortoleva 1994). Earthquakes can breach the seals between compartments (reservoirs), resulting in enhanced permeability, exchange of fluids, and redistribution of pore pressures at distances far beyond the near field (Fig. 10). Thus, sensitive soils beyond the near field can become pressurized if hydraulically connected to a high-pressure compartment by earthquakes. Liquefaction may thus occur beyond the near field at seismic energy density below the threshold for sensitive soils. Enhanced permeability between reservoirs at different pore pressures also naturally explains why changes of groundwater level in the intermediate field of an earthquake are gradual and sustained.

Material Anisotropy

Anisotropy, defined as the directional dependence of material properties, is widespread in the Earth, especially in sedimentary basins. We may thus expect that anisotropy would play an important role in affecting the hydrologic responses to earthquakes. Here we use two examples to illustrate the importance of material anisotropy in controlling earthquake-induced hydrologic responses.

Streamflow

In section "Changes in Streamflow," we showed that none of the proposed mechanisms (changes in elastic strain, enhanced horizontal permeability, and sediment consolidation) can explain the post-earthquake increase in stream discharge. As discussed in section "Earthquake-Induced Groundwater-Level Changes, aquifers in sedimentary rocks are subhorizontally layered, with relatively permeable layers (aquifers) confined between relatively impermeable ones. The effective permeability of the sandwiched structure may thus be highly anisotropic, with the effective horizontal permeability controlled by the most permeable layers and the effective vertical permeability controlled by the least permeable layers. Thus, the effective horizontal permeability is often several orders of magnitude greater than the effective vertical permeability and controls the groundwater discharge to streams (baseflow). The constancy of the recession constant before and after an earthquake (section "Changes in Streamflow") implies strictly that the effective horizontal permeability does not change appreciably after earthquakes. On the other hand, being much smaller to start with, the effective vertical permeability may be appreciably affected by a small change. Figure 11 shows a simulated post-seismic discharge based on this concept that closely fits the observation (Wang et al. 2004b).

Water-Level Change Induced by S-Waves and Love Waves

In section "Earthquake-Induced Groundwater-Level Changes," we showed that groundwater levels in Taiwan responded to the 2008 Wenchuan earthquake, more than 3,000 km away and that groundwater oscillations started substantially earlier than the arrival of the Rayleigh waves but were coincidental with the arrival of S-waves and Love waves (Wang et al. 2009; Geballe et al. 2011). Oscillation of groundwater level implies oscillatory groundwater flow, which in turn implies oscillatory volumetric strains. The Wenchuan observation is unexpected because S-waves and Love waves are commonly assumed to cause *no* volumetric changes. The fact that groundwater level in Taiwan oscillated in response to the arrival of S- and Love waves implies that this assumption may not be correct.

Detailed analysis of this problem would require knowledge of the full three-dimensional strain tensors at the well sites, which are unknown. We simply note here that while S- and Love waves cannot produce volumetric strain in isotropic solids, they do in generally anisotropic elastic solids. Since sedimentary basins are commonly anisotropic to seismic waves, it is reasonable to suggest that S- and Love waves from the Wenchuan earthquake did cause oscillatory volumetric strains in Taiwan, which, in turn, caused groundwater flow and even permanent change in permeability (Wang et al. 2009).

Effect of Seismic Wave Frequencies

Established methods of liquefaction risk analysis have been based primarily on the peak ground acceleration (*PGA*) at particular sites (e.g., Seed and Idriss 1971). *PGA* is used because it is proportional to the maximum shear stress induced in the soil (Terzaghi et al. 1996). However, a great deal of in situ evidence from earthquakes has shown that liquefied sites are characterized by low-frequency ground motions. For example, during the 1989 Chi-Chi earthquake, ground motion parameters that measure low-frequency ground motions were more strongly correlated with coseismic groundwater-level change and the occurrence of liquefaction than parameters that measure high-frequency motions (Wang et al. 2003; Wong and Wang 2007). Horizontal peak ground acceleration, a metric often used to quantify the strength of ground motion in liquefaction analysis, was weakly correlated with coseismic groundwater-level change and liquefaction, while horizontal peak ground velocity was much more strongly correlated with both. Spectral accelerations and velocities of frequencies lower than ~1 Hz were strongly correlated with the hydrologic changes, while those above ~1 Hz were not (Wang et al. 2003). Similarly, measures of earthquake intensity computed with low-pass filtered seismograms were more highly correlated with hydrologic changes than measures computed with high-pass filtered seismograms (Wong and Wang 2007). Rudolph and

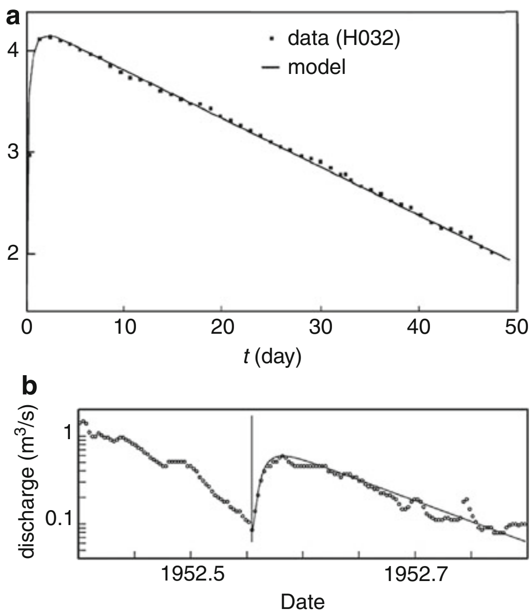

Fig. 11 (**a**) Response of a stream in central Taiwan to the 1999 M7.6 Chi-Chi earthquake. Time zero coincides with the earthquake. (**b**) Response of Sespe Creek, CA, to the 1952 M7.5 Kern County earthquake. *Vertical line* shows the time of the earthquake. *Dots* and *circles* show daily discharge measurements; *curves* show model prediction. No precipitation occurred during the time intervals in these graphs (Reproduced from Wang and Manga (2010))

Manga (2012) analyzed the response of mud volcanoes to earthquakes and found that mud volcanoes responded to the amplitude of ground velocity at low frequency, but responses were not correlated with the duration of shaking.

The consistency of this pattern across all types of seismic parameters and evaluations of correlations is convincing evidence that low-frequency motion is more strongly correlated with water-level changes and liquefaction than high-frequency motion. However, such correlations can be interpreted in different ways. One possible interpretation is that soil softening could absorb high-frequency ground motions while amplifying low-frequency motions (e.g., Youd and Carter 2005; Holzer and Youd 2007). Another possible explanation is that the low-frequency motion is the actual cause of coseismic groundwater-level changes, soil softening, and liquefaction. Results from nonlinear numerical simulations suggest that a spectrally dependent feedback loop may occur in liquefying soils (Popescu 2002; Ghosh and Madabhushi 2003), i.e., low-frequency excitation causes ground softening and pore pressure increases more efficiently than for high-frequency excitation. This softening in turn reduces the resonant frequency of the soil column, amplifying low-frequency motions and damping high-frequency motions, leading to further softening and pore pressure increases and possibly leading to liquefaction.

Dynamic Permeability

Many studies of hydrological responses to earthquake appeal to an increase in permeability induced by time-varying stresses produced by seismic waves. Increases in permeability could account for increases in stream discharge and would also redistribute pore pressure, hence causing changes in the water levels in wells.

Changes in permeability after intermediate- and far-field earthquakes have been documented in the field and in the lab. Elkhoury et al. (2006) monitored the response of water-level fluctuations produced by Earth tides and showed that phase lags in the response, whose magnitude depends on permeability, are changed by intermediate- and far-field earthquakes. The magnitude of inferred permeability changes was proportional to the amplitude of ground motion. Similar analyses after the 2008 Wenchuan earthquake show that in the near field, both permeability change and water-level change are produced by coseismic strain (Lai et al. 2014). Thus, documented hydrological responses may result from the superposition of multiple post-seismic processes.

In the laboratory, several studies have documented that strains comparable in frequency and magnitude to intermediate-field earthquakes can change permeability (Shmonov et al. 1999; Roberts 2005; Liu and Manga 2009; Beresnev et al. 2011; Elkhoury et al. 2011). While these experimental studies differ in how time-varying stresses were applied to the studied rocks, the frequency of oscillations, and the duration of shaking, they all confirm that time-varying stresses can change permeability.

Figure 12 summarizes the magnitude of permeability changes as a function of strain amplitude based on lab experiments and field studies. The magnitude of permeability changes inferred from natural field-scale studies can be orders of magnitude larger than those found in the laboratory studies. This discrepancy hints that scale effects and heterogeneity matter; the relatively homogeneous lab samples have smaller changes than at the field scale where changes in the lowest permeability units may translate to large changes in mean effective permeabilities (see section "Material Anisotropy").

The mechanism by which permeability changes at the pore scale is uncertain, but because the stresses are small, it is unlikely to involve the creation of new fractures. Instead, it is often proposed that the time variations in fluid flow produced by time variations in stress dislodge and mobilize small particles that otherwise impede fluid flow (Mogi et al. 1989; Brodsky et al. 2003). The dislodgement process could be entirely mechanical, produced by shear stresses in the pore fluid, or aided by geochemical processes which help break up particle aggregates or liberate particles adhering to grain surfaces (Roberts 2005).

Permeability changed by earthquakes recovers to values close to those prior to the earthquake (Manga et al. 2012). This occurs on time scales of minutes (Geballe et al. 2011; Elkhoury et al. 2011) to months (Elkhoury et al. 2006) to several years (Davis et al. 2001; Claesson et al. 2004, 2007; Kitagawa et al. 2007; Manga and Rowland 2009). Recovery is presumably the result of biogeochemical and mechanical processes that return the porous material to the pre-earthquake state, for example, by allowing particles to re-accumulate in the pore space.

Multiphase Flow

Subsurface porous materials can contain multiple immiscible phases: water and oil and natural gas, water and CO_2, and other combinations. The fluid flow equations for these multiphase systems are more complicated. In particular, the permeability is often modified by including a scaling factor called the relative permeability that accounts for the effects of each phase on the other. In some limits, one of the fluid phases, usually the nonwetting phase, becomes immobilized and trapped in pore space.

Mobilizing trapped drops and bubbles has the effect of increasing the relative permeability of both the continuous fluid phase and the dispersed phase. One example of a hydrological response that may result is the increase in discharge at mud volcanoes (section "Response of Mud Volcanoes). Mud volcanoes erupt a 3-phase fluid of solid sediments, water, and gas, with gas playing a key role. Rudolph and Manga (2010) invoked the mobilization of gas bubbles to explain responses of mud volcanoes to earthquakes.

The mechanism(s) through which dynamic strains and oscillating pressure gradients mobilize trapped drops and bubbles (hereafter simply called drops) has been explored experimentally

Encyclopedia of Complexity and Systems Science
DOI 10.1007/978-3-642-27737-5_606-1

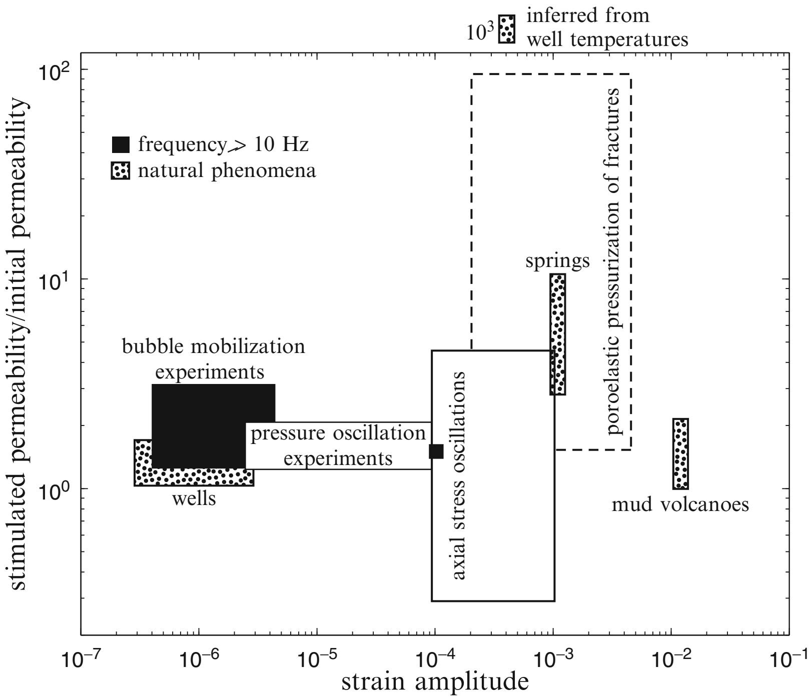

Fig. 12 Compilation of lab data and field inferences showing changes in permeability produced by oscillatory strains (Reproduced from Manga et al. (2012))

(Li et al. 2005; Beresnev et al. 2005) and with theoretical and numerical models (Graham and Higdon 2000; Beresnev 2006; Hilpert 2007; Beresnev and Deng 2010; Deng and Cardenas 2013). To be dislodged, the force acting on the drop must overcome the surface tension (capillary) forces holding the drop in place, usually at constrictions in flow paths. While this is speculative since we know of no actual data, capillary forces should act as an apparent cohesion, so changing capillary forces might have a modest effect on strengths. The passage of a seismic wave generates transient forces on, and hence pressure gradients across, trapped drops. With each cycle of motion, the drop can move at a rate controlled by the viscosity of the two phases (Deng and Cardenas 2013). Low-frequency oscillations at a given amplitude are more effective than high-frequency oscillations because the drop can move a greater distance during each cycle (Manga et al. 2012).

Mobilization of nonwetting fluids such as oil and gas by seismic stimulation has been explored for remediation of contaminated aquifers (Roberts et al. 2001) and enhancing oil recovery (Beresnev and Johnson 1994; Roberts et al. 2003).

Unsaturated vs. Saturated Flow

The presence of bubbles is generally assumed to suppress hydrological responses to earthquakes because changes in pressure (both from static and dynamic strains) can be accommodated by the high compressibility of gas (e.g., Brodsky et al. 2003). However, liquefaction does occur in gaseous sediments (Chillarige et al. 1997). In the unsaturated zone, seismic strains may influence the mobility of the wetting phase (water) by changing the connectivity and geometry of the wetting phase, hence changing relative permeability.

Observational reports of responses in the unsaturated zone are few. Manga and Rowland (2009) suggested that at least some of the excess water discharged in streams after earthquakes originated from the unsaturated zone because isotopic changes in O and H shifted towards water that experienced evapotranspiration, a process that occurs in the shallowest subsurface. Mohr et al.

(2013) documented an increase in evapotranspiration that scaled with changes in discharge, pointing to an increase in biologically available soil water and hence rising water levels. These authors suggest that seismic energy from passing seismic waves may have increased the mobility of water in the unsaturated zone, allowing it to drain to the capillary fringe and hence raise the water table.

The idea that unsaturated hydraulic conductivity may be changed by seismic waves deserves experimental study to determine whether it is a process that may explain other hydrologic responses generally attributed to processes in the saturated zone.

Practical Relevance

In the introduction we noted that in addition to being a matter of academic interest, earthquake-induced hydrologic changes also have certain practical relevance. For example, groundwater-level changes following earthquakes can affect water supplies and put some underground waste repositories at risk. Investigation of sediment liquefaction can also be useful in evaluating the eruption of mud volcanoes that can lead to massive destruction of property and lives. Furthermore, earthquake-induced groundwater flow and temperature change may have important implications for hydrocarbon maturation and migration over geologic time. In this section we discuss several examples of the practical relevance of earthquake-induced hydrologic changes.

Mud Volcano Eruptions

Most on-land mud volcanoes are either dormant or gently effusive for most of their lifetimes. However, violent paroxysms occur occasionally and represent local hazards that can damage housing and transportation infrastructure (Bonini 2009). As discussed in section "Response of Mud Volcanoes," earthquakes can trigger mud eruptions. Hence, there is interest in documenting the conditions under which a response might be expected and the possible magnitude of the response.

One dramatic example of a mud eruption, nicknamed Lusi, began in May 2006 in east Java, Indonesia (Davies et al. 2007). Eruption continues to at least the time of this writing. During the first year, the eruption rate was $> 10^5$ tons/day (Mazzini et al. 2007), and it had decreased to 10^4 t/day by 2012. This event was a devastating local disaster, displacing more than 35,000 people and causing more than $4B US in economic losses, largely through damage to infrastructure and disruption of transportation networks (Richards 2011).

Indonesia is very seismically active so it is natural to ask whether this eruption is another example of response to an earthquake. Indeed, some studies have attributed the eruption to the Yogyakarta earthquake, a magnitude 6.3 event located 250 km from the eruption site (Mazzini et al. 2007; Sawolo et al. 2009).

We can exploit the compilation of triggered mud eruptions in response to earthquakes (e.g., Manga et al. 2009) to perform a forensic analysis. Figure 13 shows that by comparison with previous examples of triggered eruptions, the Yogyakarta earthquake was much more distant than events of similar magnitude that triggered eruptions elsewhere. That is, this particular earthquake-eruption pair would have to be the most sensitive in the documented global record. A more compelling argument against an earthquake trigger, however, is that a larger and closer earthquake did not trigger an eruption (Manga 2007; Rudolph et al. 2013). In fact, at least 20 earthquakes produced larger amplitude ground motion since 1976 (Davies et al. 2008), and none of these events initiated an eruption.

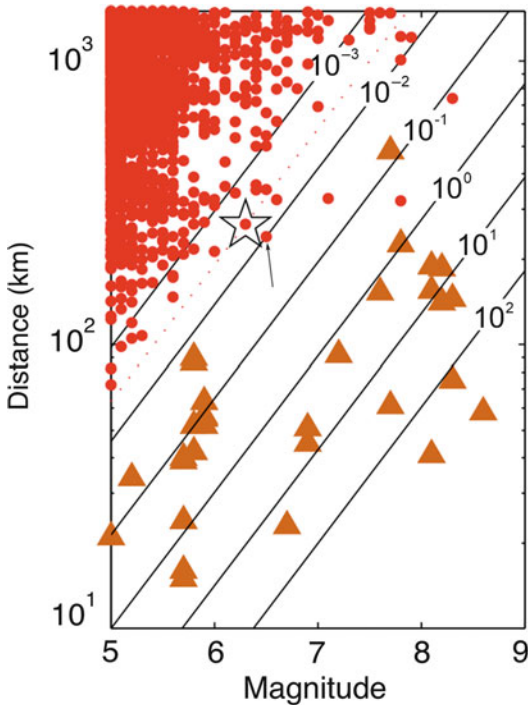

Fig. 13 Relationship between earthquake magnitude and distance between the earthquake and mud volcanoes that erupted in response (*triangles*) (Data compiled in Rudolph and Manga (2012)). The *solid lines* are lines of constant seismic energy densities in J/m^3 (Wang 2007). The *star* shows the Yogyakarta earthquake that has been implicated in the Lusi mud eruption, Indonesia. The *red circles* show all the other earthquakes since 1976 (depths less than 100 km) that did not initiate an eruption at the Lusi site – including the earthquake indicated with the *black arrow*, which was both larger and closer than the Yogyakarta event. The *red-dotted line* is the seismic energy density of the Yogyakarta earthquake

Water Resources

As shown in section "Changes in Streamflow," immediately after the Loma Prieta earthquake, stream discharge in drainage basins near the epicenter increased 4- to 24-fold (Rojstaczer and Wolf 1992). The increased discharge, however, was short lived (several months). Longer-lasting effects of earthquakes occur in areas where meltwater from snow and glaciers in high mountains is transferred to nearby valleys. Such redistribution of water caused an unexpected rise of lake level in Tibet (Yao et al. 2007), rising groundwater in the Hexi Corridor of western China (Chen and Wang 2009), and appearance of new lakes in the Taklamakan Desert (Chen et al. 2012). We use the last case to illustrate how earthquakes may have facilitated the redistribution of meltwater.

The Taklamakan Desert of northwestern China is one of the largest deserts in the world. Being far removed from the oceans and surrounded by huge mountains on all sides, the area is one of the driest on Earth. Overuse of groundwater and construction of dams on major rivers further accelerated the drying up of many lakes, including the Lop Nur. At the beginning of this century, however, some new lakes unexpectedly appeared in the desert. The origin of the water in the new lakes has been a matter of debate. Two primary hypotheses have been proposed: one is that it came from "ecological water" released from a government-implemented project. Rising water level in a large lake (the Bosten Lake) adjacent to the Tianshan Mountains during the late twentieth century, due to rising temperature and increased melting of snow and ice in the mountains, prompted the Tarim River Management Bureau to implement the Ecological Water Conveyance Project, by which water is released from the Bosten Lake intermittently to mitigate local flood condition and rescue dying riparian plants along dried riverbeds. The released water (Fig. 13) was widely assumed to be the origin of the new lakes (e.g., Wang et al. 2006; Zuo 2006). The other hypothesis is that the new water was from discharge of groundwater from nearby high mountains where increased recharge has occurred due to increased ice and snow melt.

Using isotopes of O and H as tracers, Chen et al. (2012) showed that the new lakes did not come from the Bosten Lake but may have originated from meltwater in the nearby Altyn and Kunlun Mountains. If so, how did the meltwater in the nearby mountains get to the lakes? Figure 14 shows that the lake area peaks around April of each year, three months ahead of the maximum discharge of a nearby river (the Cheerchen River). Thus the appearance of the lakes is not related to the flow in the river. Occasional rainfalls may cause flooding, but such isolated incidents cannot explain the long-term change or the annual fluctuations in the lake area.

The lack of identifiable surface water source supports the hypothesis that the source of water may be increased groundwater discharge from the nearby Altyn and Kunlun Mountains. In order for the new lakes to have originated from groundwater discharged from the nearby mountains, however, there must be enough groundwater in the mountains before the earthquakes. Mountains around the Taklamakan Desert receive little rain, and most water occurs in the forms of snow and glaciers on the high mountains. Warming climate in the past 50 years, as documented by weather stations around the Taklamakan Desert (Ma et al. 2010), may have increased melting of snow and ice in the mountains.

To further support the hypothesis, Chen et al. (2012) showed that earthquakes in the Altyn and Kunlun Mountains early in this century may have facilitated the redistribution of groundwater from the high mountains to the nearby desert. Using a first-order simulation of the increased groundwater discharge induced by the combined effect of the 2000 Ms 5.7 earthquake in the nearby Altyn Mountains and the 2001 Ms 8.1 earthquake in the Kunlun Mountains, they showed that groundwater discharge in the area of the new lakes started to increase in 2000, reached a plateau in 2003, and stayed nearly constant to year 2007, similar to the timing of the observed increase in lake area (Fig. 14a). Assuming coseismic discharge of groundwater of the order of ~1 km^3 from the mountains, as occurred after the Chi-Chi earthquake (Wang et al. 2004b), the simulated annual discharge of groundwater in the lake area between 2003 and 2006 is ~0.2 km^3, similar to the annual loss of lake water to evaporation, estimated by summing the products of monthly lake area (Fig. 14a) and monthly evaporation (Fig. 14b). This study, together with Chen and Wang (2009), shows that earthquake-induced groundwater flow may play a significant role in the redistribution of regional water resources in arid areas during a warming climate.

Subsurface Transport

It is well known that groundwater flow is effective in transporting subsurface heat and solutes (e.g., Forster and Smith 1989; Ingebritsen et al. 1989). Thus, it may be expected that large earthquakes can cause significant changes in the subsurface transport. Such effects, however, are poorly documented because of scarcity of data.

As described in section "Earthquake-Induced Groundwater-Level Changes," monitoring wells in Taiwan recorded systematic changes of groundwater temperature across a large alluvial fan after the Chi-Chi earthquake (Wang et al. 2013), providing a rare opportunity to understand earthquake-induced groundwater transport. Using numerical simulation of groundwater flow and heat transport, Wang et al. (2013) tested the hypothesis that the systematic changes of groundwater temperature may be due to earthquake- enhanced permeability that increased subsurface flow and transport. The authors first simulate groundwater flow and temperature before the earthquake (Fig. 7a), assuming steady-state conditions; these conditions were then used as the initial conditions for solving the time-

Encyclopedia of Complexity and Systems Science
DOI 10.1007/978-3-642-27737-5_606-1

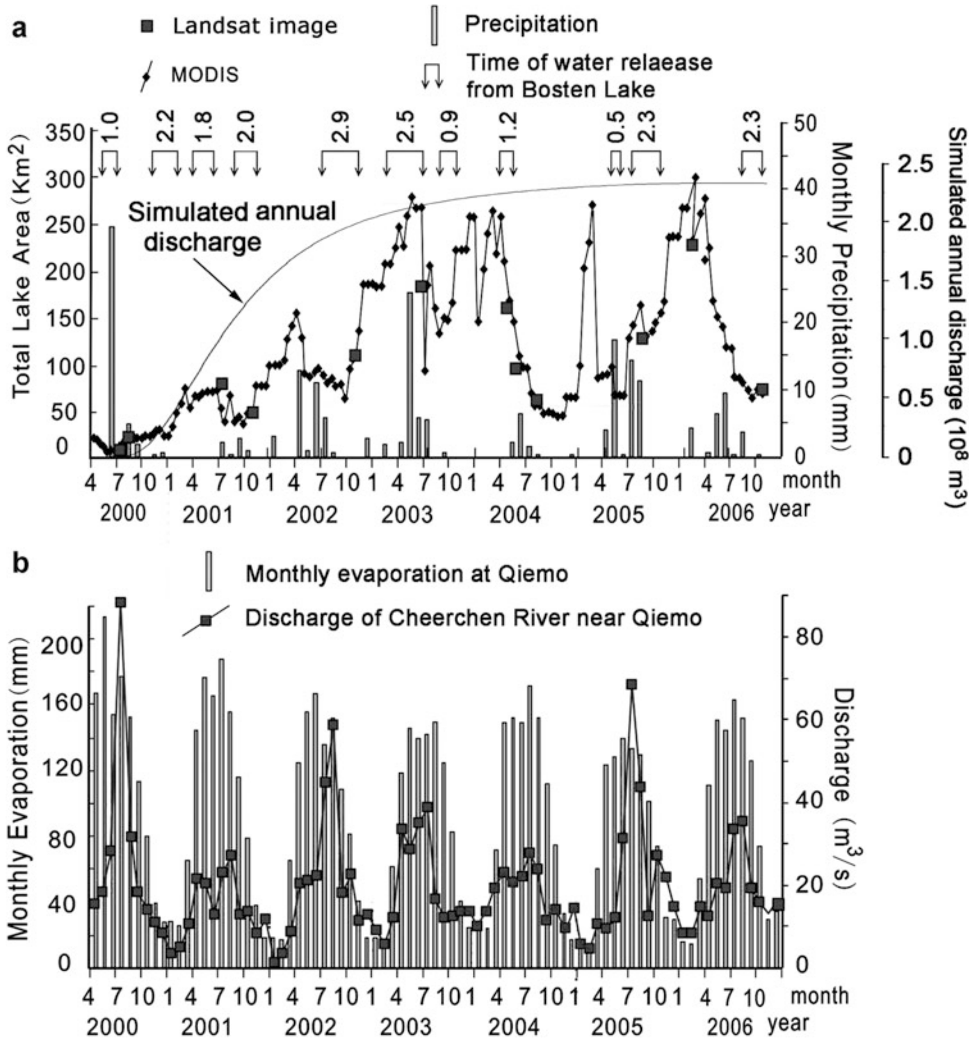

Fig. 14 (**a**) Total new lake area (Ma et al. 2008) obtained from MODIS (*diamonds*) and Landsat imageries (*squares*) plotted against time, together with monthly precipitation documented at Qiemo (Fig. 2). Notice the close agreement between the MODIS and Landsat results. The MODIS time series shows that the total lake area increased significantly from 2000 to 2003 and fluctuated annually, with increases from October to April and decreases from April to October. Precipitation occurs mostly when lake area was nearly minimum. *Brackets* show the time of water releases from Bosten Lake (Zuo 2006; Wang et al. 2006); numbers on *top* of the *brackets* show the amount of each release in 10^8 m^3. *Upper curve* shows simulated annual groundwater discharge to the lakes following the 2000 Altyn earthquake and the 2001 Kunlun earthquake (Chen et al. 2012). (**b**) Monthly discharge in the Cheerchen River and monthly potential evaporation documented at Qiemo (Reproduced from Chen et al. (2012))

dependent changes after the earthquake. Parameter sweep and optimization were used to search for the best values of permeability, in both the alluvial fan and the conglomerate formation, to fit the temperature data. Figure 7c shows that if enhanced permeability is restricted to the upper few 100 m of sediments, the simulated temperature, given by the black curve, does not change across the basin except near its ends, inconsistent with data that show gradual changes from east-to-west across the entire basin. In order to fit this gradual change in groundwater temperature after the Chi-Chi earthquake, permeability increase by several orders of magnitude must have occurred basin wide to depths of several km (Wang et al. 2013).

The result suggests that large earthquakes can enhance basin-wide transport, which may have important implications for groundwater supply and quality, contaminant transport, and underground

DOI 10.1007/978-3-642-27737-5_606-1

waste repositories. The result also suggests that the earthquake-enhanced flow extends to depths of a few km, in contrast to earlier suggestions that earthquake-enhanced groundwater flow is restricted to shallow aquifers (Rojstaczer et al. 1995; Claesson et al. 2007; Mohr et al. 2013; Wang et al. 2012). We note that while the earlier studies focused on data from a single well or small number of wells in a restricted area, Wang et al. (2013) integrated data from a large basin, so that differences in temperature are more easily recognized.

Summary and Outlook

We have discussed the complexities in the Earth's subsurface introduced by large earthquakes that change subsurface properties and groundwater flow and transport. The changes are manifest by an array of hydrological responses, ranging from changes in groundwater levels and stream discharge to liquefaction and mud volcano eruption. A common thread among the bewildering variety of responses may be the spatial distribution of seismic energy density required to trigger the different responses. On the other hand, the responses often resist a straightforward explanation due to complexities that originate from the nonlinearity, heterogeneity, and anisotropy of rocks and sediments. Other complexities may originate from dynamic changes of permeability during and following earthquakes and the responses of hydrological systems to different seismic frequencies.

Three major categories of mechanism have been proposed to explain the varieties of hydrologic responses: static poroelastic strain, undrained consolidation, and earthquake-enhanced permeability. The mechanisms are *not* mutually exclusive but may occur together and may even be causally related. For example, oscillatory flow of groundwater in the far field caused by poroelastic volumetric strain may dislodge obstacles from flow passageways and enhance permeability. Multiple mechanisms are expected to interact after an earthquake. Since different hydrologic responses are activated at different threshold seismic energy densities (section 6.2), seismic energy density high enough to activate liquefaction and mud volcano eruption, for example, must also be high enough to enhance permeability by dislodging colloidal particles from flow passageways. In other words, earthquake-enhanced permeability must occur not only in the intermediate field but also in the near field; its hydrological effect in the near field, however, may sometimes be obscured by undrained consolidation. Figure 15 shows a schematic illustration of the interaction among various hydrological responses, which is another subject largely unexplored.

Among several practical issues related to earthquake hydrology, we believe that earthquake-induced change in subsurface transport deserves particular attention. Using the widespread change in groundwater temperature in Taiwan after the Chi-Chi earthquake as an example, we showed that large earthquakes can cause basin-scale changes in groundwater transport to depths of several km. Similar changes may be common in other seismically active areas and may have important implications for groundwater supply and quality, contaminant transport, and underground waste repositories. Management plans related to these issues are based on models for pre-earthquake conditions, which may change following large earthquakes. More field studies and laboratory analysis are needed to advance this aspect of earthquake hydrology.

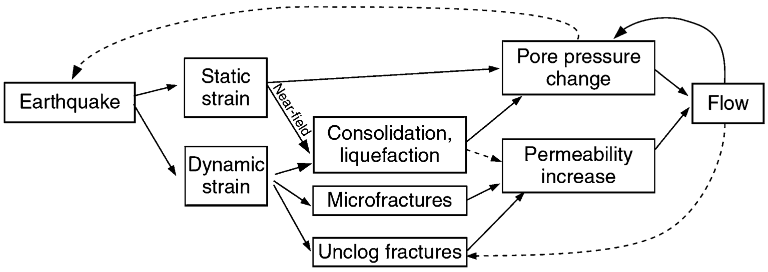

Fig. 15 Schematic illustration of the interaction among various hydrological responses to earthquake (Figure based on a drawing by David May)

Acknowledgements

We thank Steve Ingebritsen and Barbara Bekins for their excellent reviews that significantly helped us in improving the paper. This work is partially supported by NSF grant EAR-1344424 and EAR-1345125.

Bibliography

Ambraseys NN (1988) Engineering seismology, earthquake engineering. Struct Dyn 17:1–105

Bath M (1966) Earthquake energy and magnitude. Phys Chem Earth 7:115–165

Belousov A, Belousova M, Nechayev A (2013) Video observations inside conduits of erupting geysers in Kamchatka, Russia, and their geological framework: implications for the geyser mechanism. Geology. doi:10.1130/G33366.1

Beresnev IA, Johnson PA (1994) Elastic wave stimulation of oil production: a review of methods and results. Geophysics 59:1000–1017

Beresnev IA (2006) Theory of vibratory mobilization of nonwetting fluids entrapped in pore constrictions. Geophysics 71:N47–N56

Beresnev IA, Vigil RD, Li W, Pennington WD, Turpening RM, Iassonov PP, Ewing RP (2005) Elastic waves push organic fluids from reservoir rock. Geophys Res Lett 32, L13303

Beresnev IA, Deng W (2010) Viscosity effects in vibratory mobilization of residual oil. Geophysics 75:N79–N85

Beresnev IA, Gaul W, Vigil RD (2011) Direct pore-level observation of permeability increase in two-phase flow by shaking. Geophys Res Lett 38, L20302

Bonini M (2009) Mud volcano eruptions and earthquakes in the Northern Apennines and Sicily, Italy. Tectonophysics 474:723–735

Bonini M, Rudolph M, Manga M (2014) Long- and short-term triggering and modulation of mud volcano eruptions by earthquakes. Rev Geophys

Bunsen RW (1847) Physikalische Beobachtungen uber die hauptsachlichsten Geysir Islands. Annalen der Physik und Chemie 83:159–170

Brodsky EE, Roeloffs E, Woodcock D, Gall I, Manga M (2003) A mechanism for sustained groundwater pressure changes induced by distant earthquakes. J Geophys Res 108:2390. doi:10.1029/2002JB002321

Carrigan CR, King GCP, Barr GE, Bixler NE (1991) Potential for water-table excursions induced by seismic events at Yucca Mountain, Nevada. Geology 19:1157–1160

DOI 10.1007/978-3-642-27737-5_606-1

Chen J, Wang C-Y (2009) Rising springs along the Silk Road. Geology 37:243–246. doi:10.1130/G25472A.1

Chen J, Wang C-Y, Tan H, Rao W, Liu X, Sun X (2012) New lakes in the Taklamakan Desert. Geophys Res Lett 39:1–5. doi:10.1029/2012GL053985

Chia YP, Wang YS, Wu HP, Chiu JJ, Liu CW (2001) Changes of groundwater level due to the 1999 Chi-Chi earthquake in the Choshui river fan in Taiwan. Bull Seismol Soc Am 91:1062–1068

Chigira M, Tanaka K (1997) Structural features and the history of mud volcanoes in Southern Hokkaido, Northern Japan. J Geol Soc (Jpn) 103:781–791

Chillarige AV, Morgenstern NR, Robertson PK, Christian HA (1997) Seabed instability due to flow liquefaction in Fraser River delta. Can Geotech J 34:520–533

Claesson L, Skelton A, Graham C, Dietl C, MOrth M, Torssander P, Kockum I (2004) Hydrogeochemical changes before and after a major earthquake. Geology 32:641–644

Claesson L, Skelton A, Graham C, Morth C-M (2007) The timescale and mechanisms of fault sealing and water-rock interaction after an earthquake. Geofluids 7:427–440

Coussot P (1995) Structural similarity and transition from Newtonian to non-Newtonian behavior for clay-water suspensions. Phys Rev Lett 74:3971–3974

Cua GB (2004) Creating the virtual seismologist: developments in ground motion characterization and seismic early warning. PhD dissertation, Caltech

Davis EE, Wang K, Thomson RE, Becker K, Cassidy JF (2001) An episode of seafloor spreading and associated plate deformation inferred from crustal fluid pressure transients. J Geophys Res 106:21953–21963

Davies RJ, Swarbrick RE, Evans RJ, Huuse M (2007) Birth of a mud volcano: East Java, 29 may 2006. GSA Today 17:4–9

Davies RJ, Brumm M, Manga M, Rubiandini R, Swarbrick R (2008) The east Java mud volcano (2006-present): an earthquake or drilling trigger? Earth Planet. Sci Lett 272:627–638

Deng W, Cardenas MB (2013) Dynamics and dislodgment from pore constrictions of a trapped nonwetting droplet stimulated by seismic waves. Water Resour Res 49:4206–4218. doi:10.1002Iwrcr.20335

Dobry R, Ladd RS, Yokel FY, Chung RM, Powell D (1982) Prediction of pore water pressure buildup and liquefaction of sands during earthquakes by the cyclic strain method. National Bureau of Standards Building science series, 138. National Bureau of Standards and Technology, Gaithersburg, p 150

Elkhoury JE, Brodsky EE, Agnew DC (2006) Seismic waves increase permeability. Nature 411:1135–1138

Elkhoury JE, Niemeijer A, Brodsky EE, Marone C (2011) Laboratory observations of permeability enhancement by fluid pressure oscillation of in-situ fractured rock. J Geophys Res 116, B02311. doi:10.1029/2010JB007759

Etiope G, Nakada R, Tanaka K, Yoshida N (2011) Gas seepage from Tokamachi mud volcanoes, onshore Niigata Basin (Japan): origin, post-genetic alterations and CH_4-CO_2 flixes. Appl Geochem 26:348–359

Forster C, Smith L (1989) The influence of groundwater on thermal regimes of mountainous terrain: a model study. J Geophys Res 94:9439–9451. doi:10.1029/JB094iB07p09439

Galli P (2000) New empirical relationships between magnitude and distance for liquefaction. Tectonophysics 324:169–187

Ge S, Stover C (2000) Hydrodynamic response to strike- and dip-slip faulting in a half space. J Geophys Res 105:25513–25524

Geballe ZM, Wang C-Y, Manga M (2011) A permeability-change model for water level changes triggered by teleseismic waves. Geofluids 11:302–308

Ghosh B, Madabhushi SPG (2003) A numerical investigation into effects of single and multiple frequency earthquake motions. Soil Dyn Earthq Eng 23:691–704

Graham DR, Higdon JJL (2000) Oscillatory flow of droplets in capillary tubes. Part 2. Constricted tubes. J Fluid Mech 425:55–77

Green RA, Mitchell JK (2004) Energy-based evaluation and remediation of liquefiable soils. In: Yegian M, Kavazanjian E (eds) Geotechnical engineering for transportation projects. ASCE Geotechnical Special Publication, American Society of Civil Engineers, Reston, Virginia no. 126, vol 2, pp 1961–1970

Gutenberg B, Richter CF (1956) Earthquake magnitude, intensity, energy and acceleration. Bull Seismol Soc Am 46:105–145

Hill DP, Prejean SG (2007) Dynamic triggering. Treatise Geophys 4:257–291

Hilpert M (2007) Capillarity-induced resonance of blobs in porous media: analytical solutions, Lattice-Boltzmann modeling, and blob mobilization. J Colloid Interface Sci 309:493–504

Holzer TL, Tinsley JC, Hank TC (1989) Dynamics of liquefaction during the 1987 Superstition Hills, California, earthquake. Science 244:56–59

Holzer TL, Youd TL (2007) Liquefaction, ground oscillation, and soil deformation at the Wildlife Array, California. Bull Seismol Soc Am 97:961–976

Hsu CC, Vucetic M (2004) Volumetric threshold shear strain for cyclic settlement. J Geotech Geoenviron Eng 130:58–70

Hsu CC, Vucetic M (2006) Threshold shear strain for cyclic pore-water pressure in cohesive soils. J Geotech Geoenviron Eng 132:1325–1335

Husen S, Taylor R, Smith RB, Heasler H (2004) Changes in geyser eruption behavior and remotely triggered seismicity in Yellowstone National Park induced by the 2002 M 7.9 Denali fault earthquake. Geology 32:537–540

Hutchinson RA (1985) Hydrothermal changes in the upper Geyser Basin, Yellowstone National Park, after the 1983 Borah Peak, Idaho, earthquake. In: Stein RS, Bucknam RC et al (eds) USGS open file report 85-0290A, US Geological Survey, Reston, Virginia, pp 612–624

Ingebritsen SE, Sherrod DR, Mariner RH (1989) Heat flow and hydrothermal circulation in the Cascade range, north-central Oregon. Science 243:1458–1462. doi:10.1126Iscience.243.4897.1458

Ingebritsen SE, Rojstaczer S (1993) Controls of geyser periodicity. Science 262:889–892

Ingebritsen SE, Rojstaczer S (1996) Geyser periodicity and the response of geysers to deformation. J Geophys Res 101:21891–21905

Institute of Geophysics, CAS, and China Earthquake Administration (1976) China earthquake catalog. Center for Chinese Research Materials, Washington, DC, p 500 (in Chinese)

Kitagawa Y, Fujimori K, Koizumi N (2007) Temporal change in permeability of the Nojima Fault zone by repeated water injection experiments, Tectonophysics, 443, 183–192, doi:10.1016/j.tecto.2007.01.012

Koizumi N, Lai W-C, Kitagawa Y, Matsumoto Y (2004) Comment on “Coseismic hydrological changes associated with dislocation of the September 21, 1999 Chichi earthquake, Taiwan” by Min Lee et al. Geophys Res Lett 31, L13603. doi:10.1029I2004GL019897

Kopf AJ (2002) Significance of mud volcanism. Rev Geophys 40:1–52

Lai G, Ge H, Xue L, Brodsky EE, Huang F and Wang W (2014) Tidal response variation and recovery following the Wenchuan earthquake from water level data of multiple wells in the near field, Tectonophysics 619–620: 115–122.

Li W, Vigil RD, Beresnev IA, Iassonov P, Ewing R (2005) Vibration-induced mobilization of trapped oil ganglia in porous media: experimental validation of a capillary-physics mechanism. J Colloid Interface Sci 289:193–199

Liu W, Manga M (2009) Changes in permeability caused by dynamic stresses in fractured sandstone. Geophys Res Lett 36, L20307

Luong MP (1980) Stress–strain aspects of cohesionless soils under cyclic and transient loading. In: Pande GN, Zienkiewicz OC (eds) Proceeding of the international symposium of soils under cyclic and transient loading. A.A. Balkema, Rotterdam, pp 315–324

Ma MG, Song Y, Wang X (2008) Dynamically monitoring the lake group in Ruoqiang County, Xinjiang region [in Chinese with English abstract]. J Glaciol Geocryol 30:189–195

Ma R, Duan H, Hu C, Feng X, Li A, Ju W, Jiang J, Yang G (2010) A half-century of changes in China's lakes: global warming or human influence? Geophys Res Lett 37, L24106. doi:10.1029/2010GL045514

Manga M (2001) Origin of postseismic streamflow changes inferred from baseflow recession and magnitude-distance relation. Geophys Res Lett 28:2133–2136

Manga M (2007) Did an earthquake trigger the May 2006 eruption of the Lusi mud volcano? EOS 88:201

Manga M, Brodsky EE, Boone M (2003) Response of stream flow to multiple earthquakes. Geophys Res Lett 30:1214

Manga M, Brodsky E (2006) Seismic triggering of eruptions in the far field: volcanoes and geysers. Ann Rev Earth Planet Sci 34:263–291

Manga M, Brumm M, Rudolph ML (2009) Earthquake triggering of mud volcanoes. Mar Pet Geol 26(9):1785–1798

Manga M, Rowland JC (2009) Response of Alum Rock springs to the October 30, 2007 earthquake and implications for the origin of increased discharge after earthquakes. Geofluids 9:237–250

Manga M, Bonini M (2012) Large historical eruptions at subaerial mud volcanoes, Italy. Nat Hazards Earth Syst Sci 12:3377–3386

Manga M, Beresnev I, Brodsky EE, Elkhoury JE, Elsworth D, Ingebritsen S, Mays DC, Wang C-Y (2012) Changes in permeability by transient stresses: field observations, experiments and mechanisms. Rev Geophys 50, RG2004. doi:10.1029/2011RG000382

Manga M, Wang C-Y (2013) Earthquake hydrology. In: Kanamori H, Schubert G (eds) Treatise on geophysics, vol 4. Elsevier (in press)

Marler GD (1964) Effects of the Hebgen Lake earthquake on the hot springs of the Firehole, USGS Professional Paper 435, US Geological Survey, Reston, Virginia

Mazzini A, Svensen H, Akhmanov G, Aloisi G, Planke S, Malthe-Sorenssen A, Istadi B (2007) Triggering and dynamic evolution of Lusi mud volcano, Indonesia, Earth Planet. Sci Lett 261:375–388

Mellors R, Kilb D, Aliyev A, Gasanov A, Yetirmishli G (2007) Correlations between earthquakes and large mud volcano eruptions. J Geophys Res 112, B04304

Miyakawa K, Tokiwa T, Murakami H (2013) The origin of muddy sand sediments associated with mud volcanism in the Horonobe area of northern Hokkaido, Japan, G-Cubed 14, 4980–4988

Mogi K, Mochizuki H, Kurokawa Y (1989) Temperature changes in an artesian spring at Usami in the Izu Peninsula (Japan) and their relation to earthquakes. Tectonophysics 159:95–108

Mohr CH, Montgomery DR, Huber A, Bronstert A, Iroumé A, (2012) Streamflow response in small upland catchments in the Chilean coastal range to the M-W 8.8 Maule earthquake on 27 February 2010: Journal of Geophysical Research-Earth Surface, v. 117, F02032

Mohr CH, Manga M, Wang C-Y, Kirchner JW, and Bronstert A, Response of unsaturated zone to earthquakes, (submitted to Geology)

Muir-Wood R, King GCP (1993) Hydrological signatures of earthquake strain. J Geophys Res 98:22035–22068

National Research Council (1985) Liquefaction of soils during earthquakes. National Academy Press, Washington, DC, p 240

Ortoleva PJ (ed) (1994) Basin compartments and seals. AAPG Memoir 61. American Association of Petroleum Geologists, Tulsa

Papadopoulos GA, Lefkopulos G (1993) Magnitude-distance relations for liquefaction in soil from earthquakes. Bull Seismol Soc Am 83:925–938

Pitilakis KD (ed) (2007) Earthquake geotechnical engineering. Springer, Dordrecht

Popescu R (2002) Finite element assessment of the effects of seismic loading rate on soil liquefaction. Canadian Geotech J 29:331–334

Pliny 79 is translated as Pliny the Elder, 1855, the natural history of Pliny (translated from Greek, by Bostock J, Riley HT, Bohn HG). London

Quigley MC, Bastin S, Bradley BA (2013) Recurrent liquefaction in Christchurch, New Zealand, during the Canterbury earthquake sequence. Geology 41:419–422. doi:10.1130/G33944

Richards JR (2011) Report into the past, present, and future social impacts of Lumpur Sidoarjo. Humanitas Sidoarjo Fund, Melbourne, Victoria, Australia, 181 pages

Rinehart JS (1980) Geysers and geothermal energy. Springer, New York, p 222

Rinehart JS, Murphy A (1969) Observations on pre- and post-earthquake performance of old faithful geyser. J Geophys Res 74:574–575

River Geyser Basins, Yellowstone National Park, USGS Professional Paper 435Q, 185197

Roberts PM (2005) Laboratory observations of altered porous fluid flow behavior in Berea sandstone induced by low-frequency dynamic stress stimulation. Acoust Phys 51:S140–S148

Roberts PM, Sharma A, Uddameri V, Monagle M, Dale DE, Steck LK (2001) Enhanced DNAPL transport in a sand core during dynamic stress stimulation. Environ Eng Sci 18:67–79

Roberts P, Esipov IB, Majer EL (2003) Elastic wave stimulation of oil reservoirs: promising EOR technology? Lead Edge 22:448–453

Roeloffs EA (1998) Persistent water level changes in a well near Parkfield, California, due to local and distant earthquakes. J Geophys Res 103:869–889

Rojstaczer S, Wolf S (1992) Permeability changes associated with large earthquakes: an example from Loma Prieta, California, 10/17/89 earthquake. Geology 20:211–214

Rojstaczer S, Wolf S, Michel R (1995) Permeability enhancement in the shallow crust as a cause of earthquake-induced hydrological changes. Nature 373:237–239

Rudolph ML, Manga M (2010) Mud volcano response to the April 4, 2010 El Mayor- Cucapah earthquake. J Geophys Res 115, B12211. doi:10.1029/2010JB007737

Rudolph ML, Manga M (2012) Frequency dependence of mud volcano response to earthquakes. Geophys Res Lett 39(14), L14303

Rudolph ML, Shirzaei M, Manga M, Fukushima Y (2013) Evolution and future of the Lusi mud eruption inferred from ground deformation. Geophys Res Lett 40(6):1089–1092

Sawolo N, Sutriono E, Istadi BP, Darmoyo AB (2009) The LUSI mud volcano triggering controversy: was it caused by drilling? Mar Pet Geol 26:1766–1784

Seed HB (1968) Landslides during earthquakes due to soil liquefaction. J Soil Mech Found Div ASCE 94:1053–1122

Seed HB, Lee KL (1966) Liquefaction of saturated sands during cyclic loading. J Soil Mech Found Div 92:105–134

Seed HB, Idriss IM (1971) Simplified procedure for evaluating soil liquefaction potential. J Soil Mech Found Div 97:1249–1273

DOI 10.1007/978-3-642-27737-5_606-1

Shi Z, Wang G, Wang C-Y, Manga M, Liu C, Liu C, Yang X (2014) Hydrological changes in response to the Wenchuan and Lushan earthquake. Earth Planet Sci Lett (in press)

Shmonov VM, Vitovtova VM, Zharikov AV (1999) Experimental study of seismic oscillation effect on rock permeability under high temperature and pressure. Int J Rock Mech Min Sci 36:405–412

Silver PG, Vallette-Silver NJ (1992) Detection of hydrothermal precursors to large northern California earthquakes. Science 257:1363–1368

Steinberg GS, Merzhanov AG, Steinberg AS, Rasina AA (1982a) Geyser process: its theory, modeling, and field experiment, part 2. A laboratory model of a geyser. Mod Geol 8:71–74

Steinberg GS, Merzhanov AG, Steinberg AS (1982b) Geyser process: its theory, modeling, and field experiment, part 3. On metastability of water in geysers. Mod Geol 8:75–78

Terzaghi K (1925) Erdbaummechanic. Franz Deuticke, Vienna

Terzaghi K, Peck RB, Mesri G (1996) Soil mechanics in engineering practice, 3rd edn. Wiley, New York, p 195

U.S. Department of Energy (2010) Complex systems science for subsurface fate and transport, DOE/SC-0123

Vucetic M (1994) Cyclic threshold of shear strains in soils. J Geotech Eng 120:2208–2228

Wang C-H, Wang C-Y, Kuo C-H, Chen W-F (2005) Some isotopic and hydrological changes associated with the 1999 Chi-Chi earthquake, Taiwan. Island Arc 14:37–54

Wang C-Y (2007) Liquefaction beyond the near field. Seismol Res Lett 78:512–517

Wang C-Y, Cheng LH, Chin CV, Yu SB (2001) Coseismic hydrologic response of an alluvial fan to the 1999 Chi-Chi earthquake, Taiwan. Geology 29:831–834

Wang C-Y, Dreger DS, Wang C-H, Mayeri D, Berryman JG (2003) Field relations among coseismic ground motion, water level change, and liquefaction for the 1999 ChiChi (Mw = 7.5) earthquake, Taiwan. Geophys Res Lett 30:1890. doi:10.1029/2003GL017601

Wang C-Y, Wang C-H, Kuo C-H (2004a) Temporal change in groundwater level following the 1999 (Mw = 7.5) Chi-Chi earthquake (1999), Taiwan. Geofluids 4:210–220

Wang C-Y, Wang CH, Manga M (2004b) Coseismic release of water from mountains: evidence from the 1999 (Mw = 7.5) Chi-Chi earthquake. Geology 32:769–772

Wang C-Y, Wong A, Dreger DS, Manga M (2006) Liquefaction limit during earthquakes and underground explosions – implications on ground-motion attenuation. Bull Seismol Soc Am 96:355–363

Wang C-Y, Chia Y (2008) Mechanism of water level changes during earthquakes: near field versus intermediate field. Geophys Res Lett 35, L12402. doi:10.1029/2008GL034227

Wang C-Y, Chia Y, Wang O-L, Dreger D (2009) Role of S waves and Love waves in coseismic permeability enhancement. Geophys Res Lett 36, L09404. doi:10.1029/2009GL037330

Wang C-Y, Manga M (2010) Earthquakes and water. Lecture notes in earth sciences, vol 114. Springer, Berlin, p 218

Wang C-Y, Manga M (2011) Hydrologic responses to earthquakes – a general metric. In: Yardley B, Manning C, Garven G (eds) Frontiers in geofluids. Wiley-Blackwell, Oxford, pp 206–216

Wang C-Y, Manga M, Wang C-H, Chen C-H (2012) Earthquakes and subsurface temperature changes near an active mountain front. Geology 40:119–122

Wang C-Y, Wang L-P, Manga M, Wang C-H, Chen C-H (2013) Basin-scale transport of heat and fluid induced by earthquakes. Geophys Res Lett 40:1–5. doi:10.1002/grl.50738

Wang R, Sun Z, Gao Q (2006b) Water level change in Bosten Lake under the climatic variation background of central Asia around 2002 (in Chinese with English abstract). J Glaciol Geocryol 28:324–329

DOI 10.1007/978-3-642-27737-5_606-1

Wells DL, Coppersmith KJ (1994) New empirical relationships among magnitude, rupture length, rupture width, rupture area, and surface displacement. Bull Seismol Soc Am 84:974–1002

West M, Sanchez JJ, McNutt S (2005) Periodically triggered seismicity at Mount Wrangell, Alaska, after the Sumatra earthquake. Science 308:1144–1146

White DE (1967) Some principles of geyser activity, mainly from Steamboat Springs, Nevada. Am J Sci 265:641–684

Wiesner M (1999) Morphology of particle deposits. J Environ Eng 125:1124–1132

Wong A, Wang C-Y (2007) Field relations between the spectral composition of ground motion and hydrological effects during the 1999 Chi-Chi (Taiwan) earthquake. J Geophys Res 112, B10305. doi:10.1029I2006JB004516

Yao T, Pu J, Lu A, Wang Y, Yu W (2007) Recent glacial retreat and its impact on hydrological processes on the Tibetan Plateau, China, and surrounding regions. Arct Antarct Alp Res 39:642–650

Youd TL, Carter BL (2005) Influence of soil softening and liquefaction on spectral acceleration. J Geotech Geoenviron Eng 131:811–825

Zeghal M, Elgamal A-W (1994) Analysis of site liquefaction using earthquake records. J Geotech Eng 120:996–1017

Zuo QT (2006) Effect and risk of ecological water transportation from Bosten Lake to Tarim River (in Chinese with English abstract). Sci Geogr Sinica 26:564–568